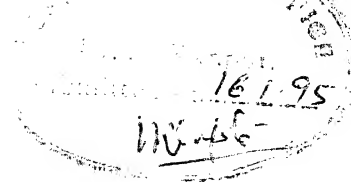# EXPERIMENTAL INVESTIGATIONS FOR THE ENHANCEMENT OF ECDM PROCESS CAPABILITIES USING VARIOUS TOOL KINEMATICS

A Thesis Submitted

in Partial Fulfillment of the Requirements

for the Degree of

Master of Technology

by

Naveen Gautam

to the

DEPARTMENT OF MECHANICAL ENGINEERING

INDIAN INSTITUTE OF TECHNOLOGY KANPUR

KANPUR 208016, INDIA

January 1995

It is certified that work contained in the thesis entitled EXPERIMENTAL INVES-
TIGATIONS FOR THE ENHANCEMENT OF ECDM PROCESS CAPABILITIES USING
VARIOUS TOOL KINEMATICS, by Naveen Gautam, has been carried out under my
supervision and that this work has not been submitted elsewhere for a degree.

January 1995

Prof. V. K. Jain

Department of Mechanical Engineering

I.I.T. Kanpur

ME- 1995- M - GAU - EXP

TH
620.14
G8352

SYNOPSIS

Electrically non-conducting ceramic materials are becoming increasingly popular because of their inert nature, high hardness and refractoriness. Traditional machining processes and a few of more common non-traditional machining methods such as, ECM and EDM, can not be used for the machining of this class of materials. Electro-chemical discharge machining (ECDM) was found to be a potential process for machining of these materials. However, ECDM it self has got its own problems, such as, limiting depth characteristic, upward shifting of discharge zone during machining, and size limitation for hole in case of drilling operation. So far, only solid non-rotational tools have been used by previous researchers. However, their findings have not been very encouraging. In the present work different tool kinematics like stationary tool and rotational tool with or without electrolyte flow through it, tool with orbital rotation, and upward movement of the work for feed in place of downward gravity feed to the tool have been used. For this purpose an experimental electro-chemical discharge drilling machine has been designed and fabricated. Experiments have been performed with borosilicate glass, quartz and alumina as work materials.

Rotation of the tool and flow of the electrolyte have improved the process performance. However, in both the cases, the maxima is attained at their low values and, beyond which any further increase in speed or electrolyte flow have adversely affected the process performance. Significant improvement in the limiting value of the machined depth was observed during orbital ECDM without sacrificing the machined surface quality. Geometrical parameters such as taper angle and circularity error have also been studied and presented. Surface integrity of the holes obtained after ECDM have also been analyzed using scanning electron microscope.

ACKNOWLEDGEMENTS

(Naveen Gautam)

DEDICATED TO

MY PARENTS

Contents

.

List of Figures

List of Tables

Chapter 1

INTRODUCTION

1.1   An Overview of Machining of Electrically Non-conducting Materials

Machining has always played an important role in shaping not only materials but in fact the fate of the humanity. This is so because machining has a special status in the whole spectrum of all manufacturing processes. The reasons behind this are the following capabilities of machining:

1. High accuracy and finish can be achieved;

2. Complex shapes can be produced;

3. Small number of parts can be produced economically;

4. The properties of the bulk of the work material remains unchanged.

Manufacturing remained a craft till the last quarter of the eighteenth century when the first industrial revolution led to a total transformation of the concepts and practices and machining became an art. With growing importance and increasing interest taken by researchers working in the field of machining, in the beginning of the current century it ultimately acquired a status of science. However, material removal

by chipping and plastic deformation, remained as the only way of removal of excess material in all types of machining processes. Recent advances in the science and technology specially in the areas like nuclear and aerospace engineering have imposed a severe demand on the material requirements. As a result of this, metallurgists and material scientists have been continuously developing newer and larger varieties of high quality materials. These materials are of increasingly higher strength, higher hardness and difficult to machine. The advent of such high strength, temperature resistant, hard and brittle materials posed serious problems to the manufacturing industry. This led to the development of entirely new methods of machining using the principles underlaying some of the new physical phenomena uncovered and studied since the beginning of the twentieth century. Such processes are grouped under the common heading 'un-conventional machining ' or 'non-traditional machining'.

Fig 1.1 shows the schematic representation of various non-conventional machining methods. However, these un-conventional machining processes also have their own limitations. The most capable un-conventional machining processes like electrochemical machining and electric discharge machining can not be applied for machining of the electrically non-conducting materials.

Fig 1.2 shows the specific electrical conductivities of various materials. It is clear from the figure that most of the high performance ceramic materials are out of the range of the ECM and EDM processes. Ultrasonic machining (USM), abrasive jet machining (AJM), laser beam machining (LBM), electron beam machining (EBM) and ion beam machining(IBM) are those processes which can be applied to hard, brittle and electrically non-conducting materials.

3
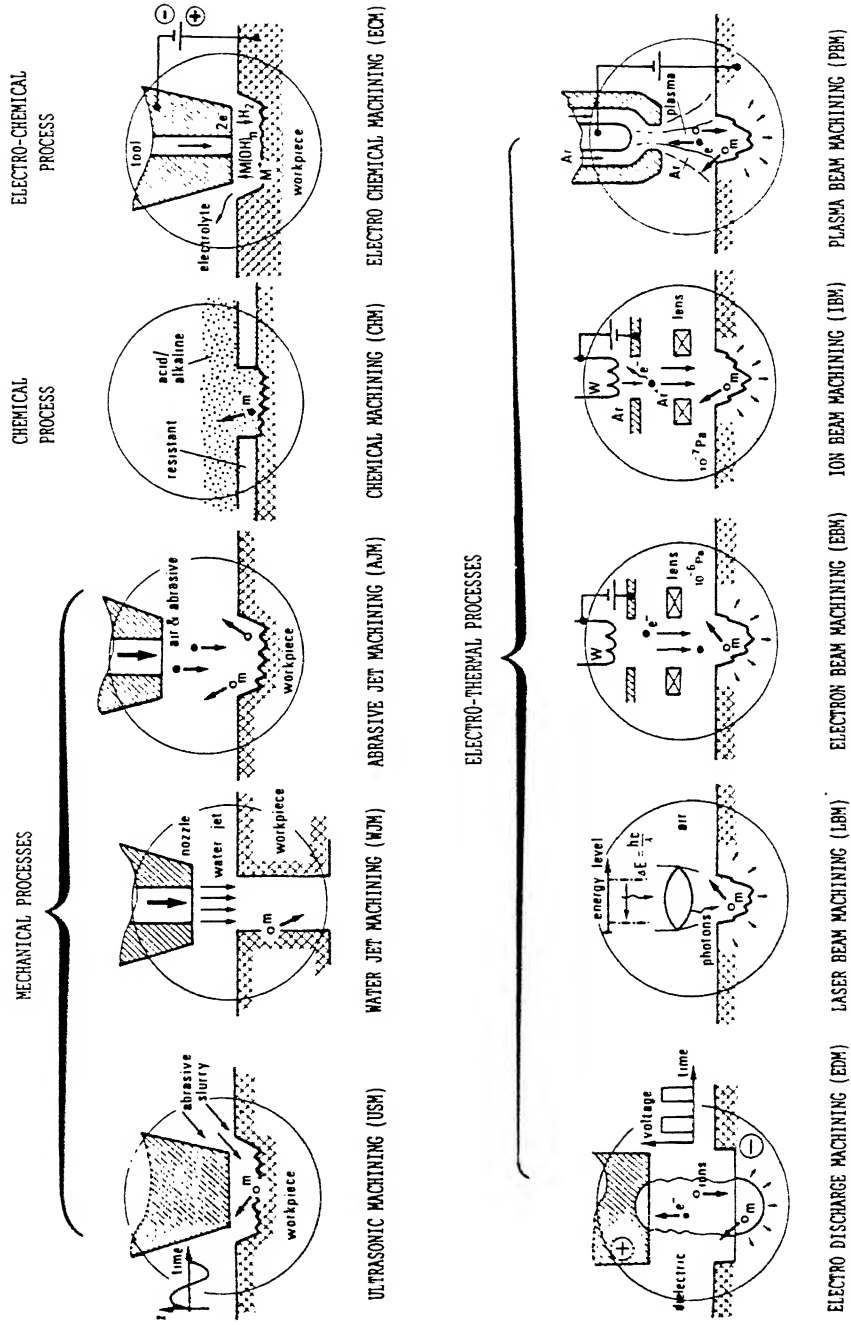
Figure 1.1: Models showing various non-conventional machining methods [31]
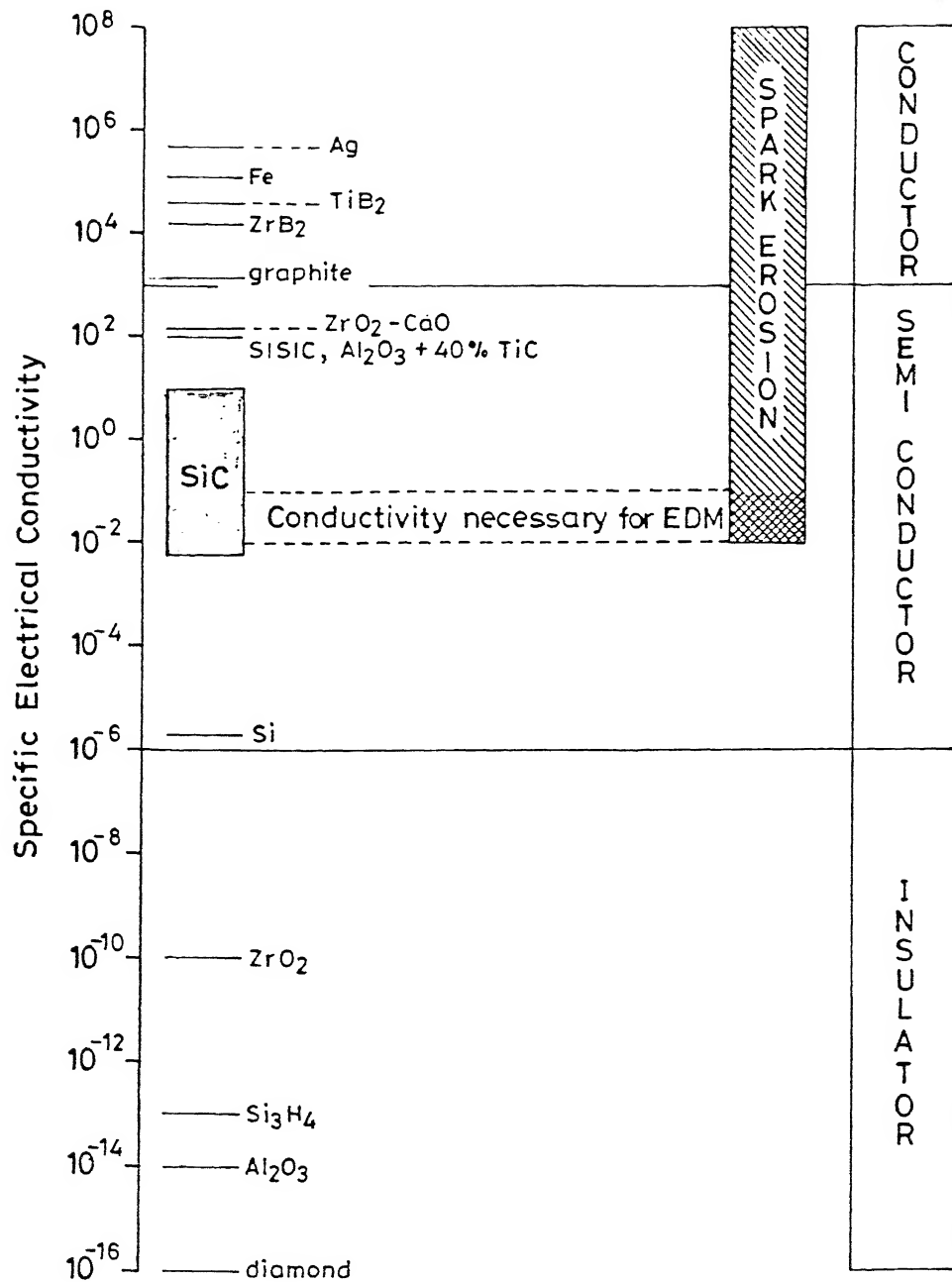
Figure 1.2: specific electrical conductivities of the various materials [15]

Production of non-conducting materials such as glass and ceramic parts needs not only the complicated manufacturing processes such as casting, compacting, melting, forming and sintering, but also the machining processes such as drilling, grinding and polishing, according to the required shape and accuracy. However, for the production of small number of parts or diversified application of these materials, it is not economically viable to use the mass production techniques such as casting and sintering. However, because of the fact that it is generally difficult to work with these materials which are brittle, hard and non-conductive, the fields for utilization of these materials might have been remained restricted. So, an attempt has been made to exploit the potential of the electrochemical discharge phenomenon for the machining of the non-conducting hard and brittle materials using various tool kinematics. Tool kinematics is defined as the branch concerned with the of motion of tool with out reference to mass and force.

1.2   Introduction to Electrochemical Discharge (ECD) Phenomenon

A simple electrochemical cell consists of two electrodes dipped in an electrolyte (Fig. 1.3 a). When an external potential is applied between the electrodes, electrical current flows through a cell resulting in electrochemical reactions such as anodic dissolution, cathodic deposition, electrolysis of electrolyte etc, depending on the electrode - electrolyte combination. Electrolytic cell can exhibit any one of the following three different phenomena namely, electrochemical action only (as in normal ECM), electrochemical action followed by discharge between the electrodes or electrochemical action followed by discharge between an electrode and electrolyte (ECD). If a suitable electrolyte is chosen and the electrodes are of grossly different

sizes (Fig. 1.3 b) then, beyond a certain value of the applied potential, electric sparks appear at the smaller electrode and the cell current drops. This is known as Electro-Chemical Discharge (ECD) phenomenon. When a non-conducting material is placed in the close vicinity of this sparking zone, material can be removed. This type of machining is known as Electro-Chemical Discharge Machining (ECDM).

1.3 Mechanism of Electrochemical Discharge Phenomenon

The mechanism of ECD, by and large, is not well defined. Though the observations of this process have established the fact that the discharge takes place across the bubbles which may be generated due to electro-chemical action and electrolyte vaporization.

Electrochemical action with electrical discharge between one electrode and electrolyte kind of situation arises when a sufficiently high electric field exists across a gas bubble or a non conducting layer in an electrochemical setup. In fact, this phenomenon occurs when two electrodes of grossly different sizes are placed apart from each other. The blanketing of the tool electrode has been identified as the primary reason for discharge initiation. The blanketing of the tool takes place due to the generation of hydrogen gas from electrochemical reaction and water vapour formation due to interface boiling of the electrolyte. Any electrical circuit consists of elements such as resistance, capacitance and inductance. The constriction of current due to bubble formation causes nonuniformity in the current path and results in an inductive effect apart from the resistive one. Thus, the circuit of an ECD setup can be represented as shown in figure 1.4. Referring to this figure C_1 and L are the capacitance and inductance respectively which are the inherent parameters
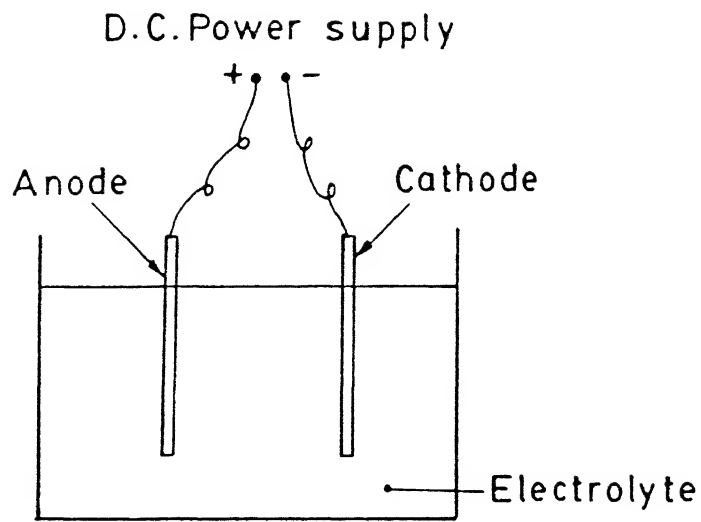
(a) Electrochemical cell
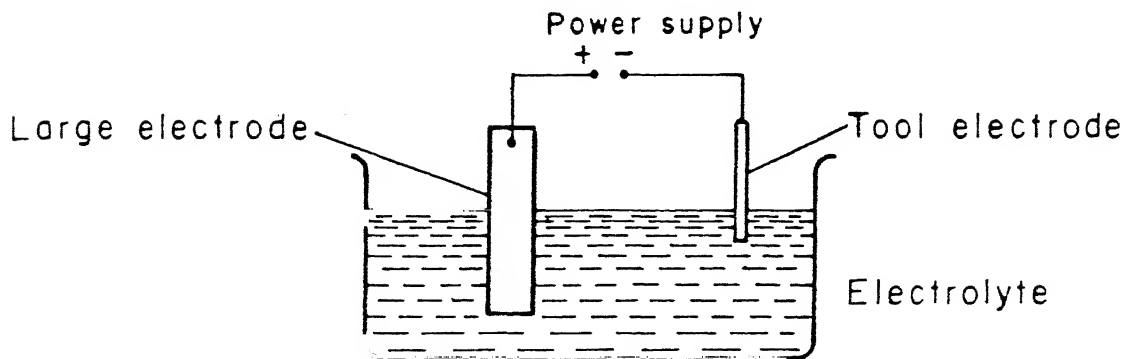
(b) schematic diagram of ECD set up

Figure 1.3

of the circuit. C_2 and C_3 are the capacitance values of the interfaces which arise due to the accumulation of the opposite charges in the regions. R_1 and R_3 are the resistances at the interfaces due to the constriction effect of the bubbles and R_2 is the resistance due to bulk electrolyte.

When the nucleation site density of hydrogen becomes sufficiently high, substantial constriction of the current path takes place at the interface. This causes an increased resistance at the region and the ohmic heating of the electrolyte becomes significant. This further causes the onset of vapour bubbles in addition to that of hydrogen bubbles. With the increase in the size of bubbles at the same stage, the point of contact between the electrolyte and tool, known as bubble bridge, blows off instantaneously due to intense heating. Consequently, the current through the circuit drops to zero within a very short time span, which is analogous to the switching off in an electrical circuit and discharge takes place along the locations of the bubble bridges. The bubbles dislodge from the electrode surface due to bridge blowing and the contact between the electrode is reestablished. This cycle repeats continuously.

1.4   Electro-Chemical Discharge Machining of non conductors

The configuration of machining of non conducting materials is shown in figure 1.5. Tool is one electrode and the second electrode is simply kept in the electrolyte at some distant location. Tool is in contact with the work and the tool feed is provided by the gravity.

When the voltage (say, 60 volts) is applied, sparks are produced at the tool and the material from the non-conducting work gets thermally eroded. There is no discharge at the non-machining electrode with the electrolyte. MRR depends
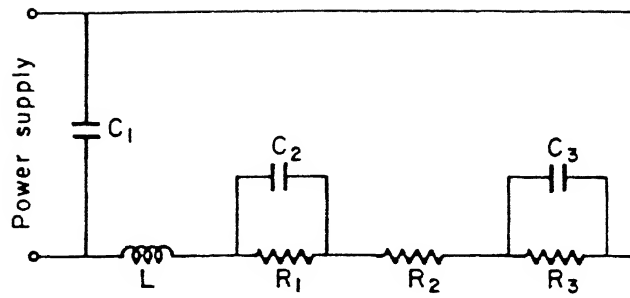
Figure 1.4: Equivalent electrical circuit of ECD set up
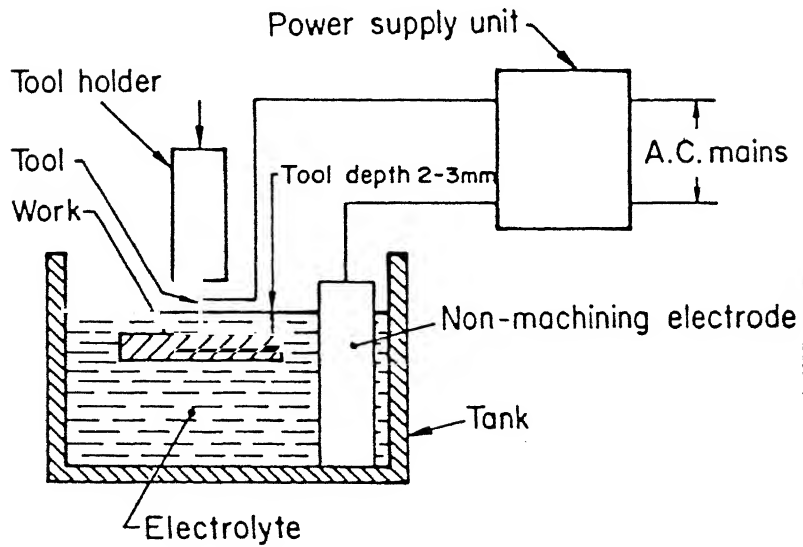
Figure 1.5: Configuration of non-conducting work machining using ECDM [3]
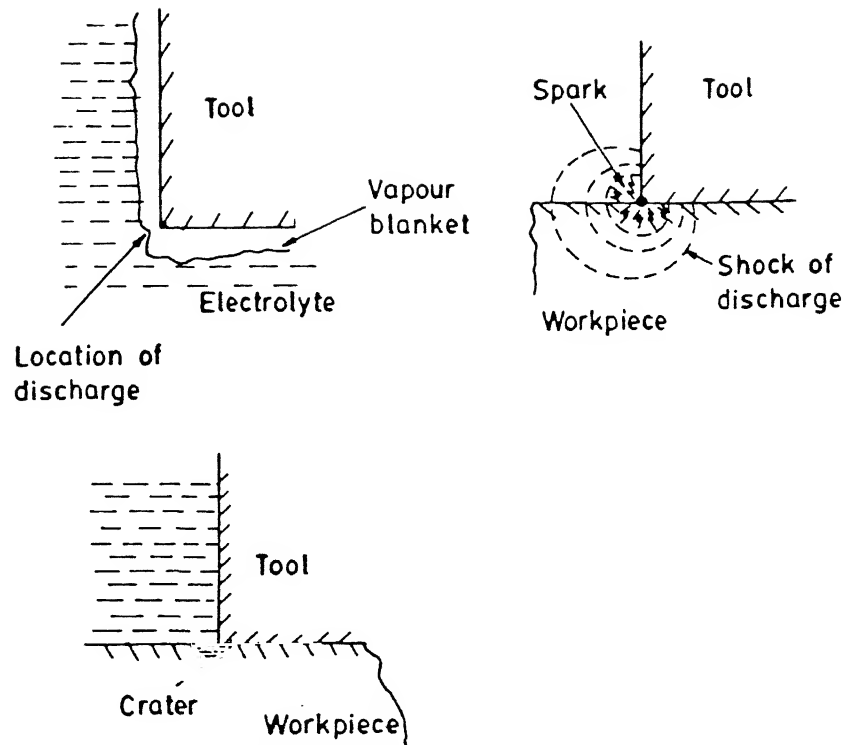
Figure 1.6: Mechanism of material removal in ECDM [3]
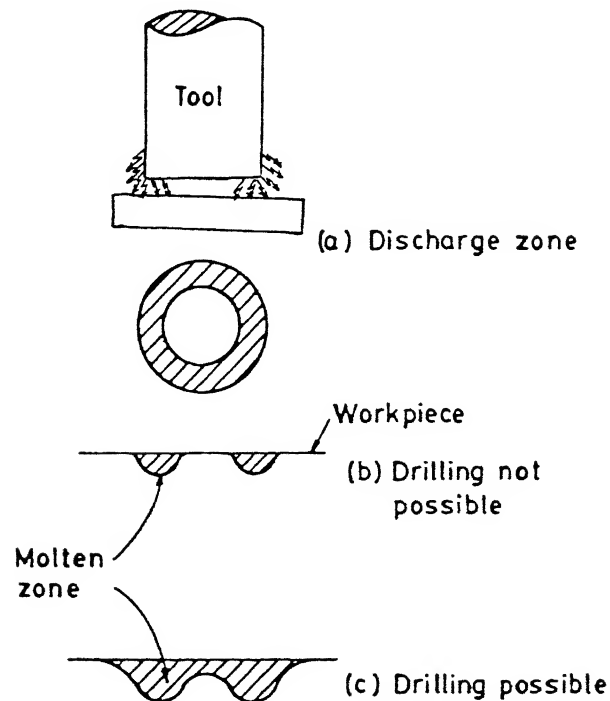
Figure 1.7: Drilling by ECDM [3]

mainly on applied voltage, electrolyte type, its temperature and concentration, tool polarity, type of power supply, work material etc.

The basic mechanism, suggested by various researchers [1,3,8,35], of material removal in ECDM is a thermal erosion. A part of the energy released by a discharge is conducted into the work piece and rises its temperature to a high value. This temperature rise is constrained to a localized region. If the highest temperature attained in this region is more than the melting temperature of the work piece, a part of the work piece melts. This molten material is removed by shock waves formed due to the discharge and ultimately a small crater is formed. The mechanism of metal removal in ECDM is some what comparable with that of the electric discharge machining (EDM).

Schematic diagram of initiation of discharge and material removal in ECDM is shown in figure 1.6. During experimentation, it was observed that sparking zone is a small area in the vicinity of the edge (Fig.1.7 a). With the increased applied voltage, the region of sparking enlarges and the vacant area at the center shrinks. Simultaneously, the sparking zone also spread along the side of the tool. The molten part of the work piece surface is indicated in figure 1.7 (b) and 1.7 (c). In figure 1.7 (b), the distribution of the temperature at the work piece material is such that at the central region, no melting takes place. This unmelted region restricts the penetration of the tool in the work piece and the machining becomes difficult. The width of the annular area of the discharge expands towards the central region with increased current, i.e. with increased applied voltage. Also, the energy density of the sparking zone increases with applied voltage. When the molten areas overlap at the central region, the tool can move downward in the work piece and then, the

drilling can be done. But, at higher applied voltage, tool and machined surfaces are badly damaged. With the larger diameter tool, ECDM is not possible as the molten areas never overlap. However solution for this problem is discussed in section 4.7.

1.5 Literature Survey

Electrical discharge between tool and work piece was observed during the attempts of enhancing the MRR in ECM by the application of higher voltage [21]. This phenomenon was considered as a detrimental one, as it causes damage to the tool and work both. The phenomenon of electric discharge in electrolyte was first utilized by Kurafugi and Suda [17]. They drilled holes up to the depth of 0.31 mm in a glass work piece (15% NaOH electrolyte with a cell voltage of 34 volts).

Cook, Foot, Jordan and Kalyani [8] have studied the ECDM of glass. They found the process to be polarity dependent and electrolyte sensitive. Machining rate increases both with concentration and temperature of electrolyte, but for a given voltage the rate of machining was found to decrease with time. They suggested that the possible mechanism of metal removal in ECDM could be attributed to the thermomechanical, chemical, electric field effect and due to some other unknown effects. A pulsed D.C. supply was also used to test the effect of high frequency pulsed current. It was found that for pulsed power supply, with pulses in micro second range, MRR increased by a factor of two. Also, surface produced by pulsed power was found to be much smoother than that from a D.C. power supply.

Loutrel and Cook [20] discussed the methods of increasing MRR in ECM, both experimentally as well as analytically. According to them, an arc in ECM occurs when a sufficiently high voltage gradient causes breakdown of hydrogen gas bub-

bles. They predicted that arcs are always formed across the voids. If the voltage gradient across the void exceeds the dielectric strength or breakdown voltage, an arc occurs. Once the arc is initiated, it may either die or grow larger. In extreme machining conditions, the arc continues to grow, bridges the gap and causes wear of the electrode-surfaces. This is a typical failure point. Loutrel and Cook suggested following seven mechanisms leading to high voltage gradient in the presence of voids:

1. Electrolytic gas evolution at electrode surface,

2. Depletion layers,

3. Electrode passivation and activation over voltages,

4. Local stagnation of flow,

5. Steam generation and cavitation,

6. Vapour blanketing of electrode surface,

7. Particles in electrolyte flow.

Tsuchiya et al. [34] used wire electrochemical discharge for machining of glass and ceramics. The cutting technique of wire EDM combined with the mechanism of ECDM has been the basis of machining . They used 25 Hz rectangular pulse with 80% duty factor, NaOH and KOH as electrolyte, glass specimen of 1.2 mm thickness as work piece, wire of diameter 0.2 mm as electrode with speed of 60 cm/min in the experiments.

Umesh Kumar [35] studied ECSM of non-conducting materials with negative tool. The results obtained are given in figure 1.8. He noticed that the discharge

vanished practically with flowing electrolyte. He suggested the mechanism of material removal as thermo-mechanical and electro-chemical actions.

Allesu [1] studied ECDM phenomenon for micro welding and engraving processes. He suggested that the mechanism of material removal depends on thermal heating, cavitation and electro-chemical action. He reported discharge voltage to increase with increase in flow velocity (Fig. 1.9 a). He also discussed the possible distribution of voltage drop in ECDM (Fig. 1.9 b). Allesu explained the reason for limiting depth characteristic as a result of loss of potential between the tool electrode and bulk electrolyte with the tool penetration in the work piece (Fig. 1.9 c). He further explained the cause of potential loss as the accumulation of gas bubbles, machined chips and electrolyte under confined condition inside the hole. The conductivity of such a three phase mixture is always far less than the conductivity of bubble free electrolyte. Therefore, the potential available between tool and electrolyte decreases with increase in machined depth. He also observed upward shifting of the discharge zone in drilling operation using ECDM (Fig.1.9 d). This phenomenon is observed during the machining due to downward motion of tool. In the present study this problem is avoided by the use of work feed mechanism (Sec. 2.1.1), so that the tool depth inside the electrolyte remains constant through out the machining. Tool coatings were also tried by him but all coatings went away very soon in discharging situation.

Tandon et al. [32] conducted two types of experiments, viz. cutting of glass-epoxy composites and drilling circular blind holes in kevlar-epoxy composites. They reported increase in MRR, TWR and overcut with increase in voltage and electrolyte conductivity, and with decrease in tool diameter. Fiber volume fraction was reported
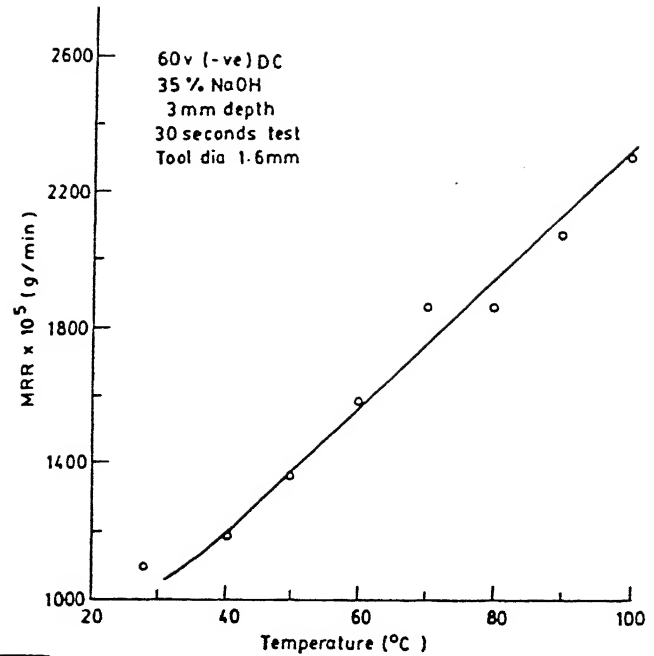
Effect of the temperature of electrolyte on material removal rate (work material: glass)
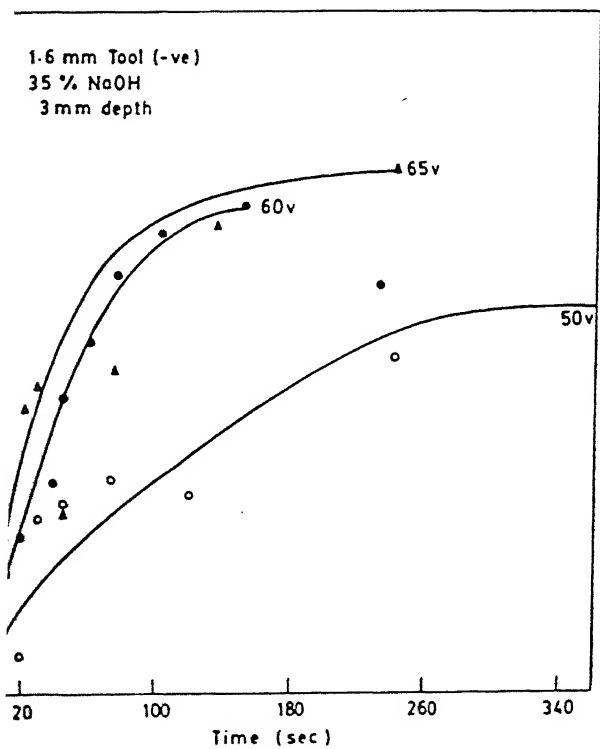
Limited depth characteristics   (work material: glass)
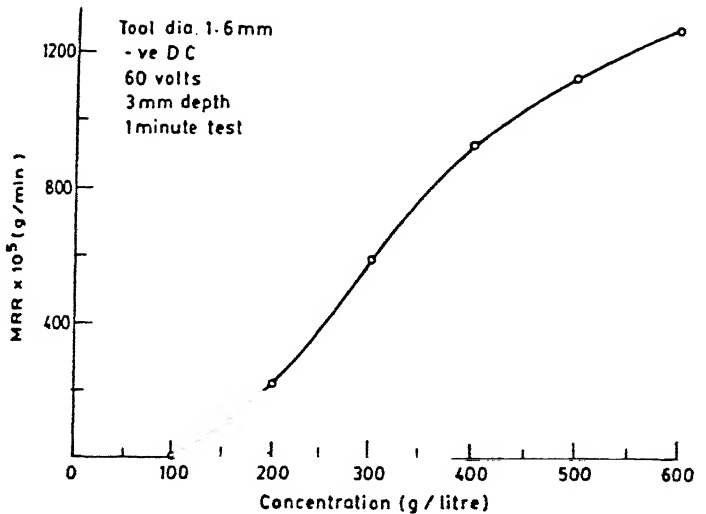
Effect of the concentration of electrolyte (NaOH) on material removal rate (work material: glass)

Figure 1.8: Parametric study during ECDM [35]
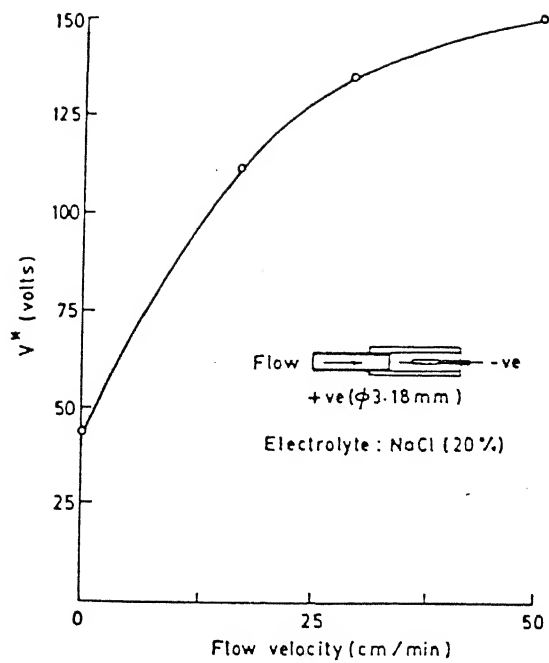
Effect of the electrolyte flow on V^* [1]
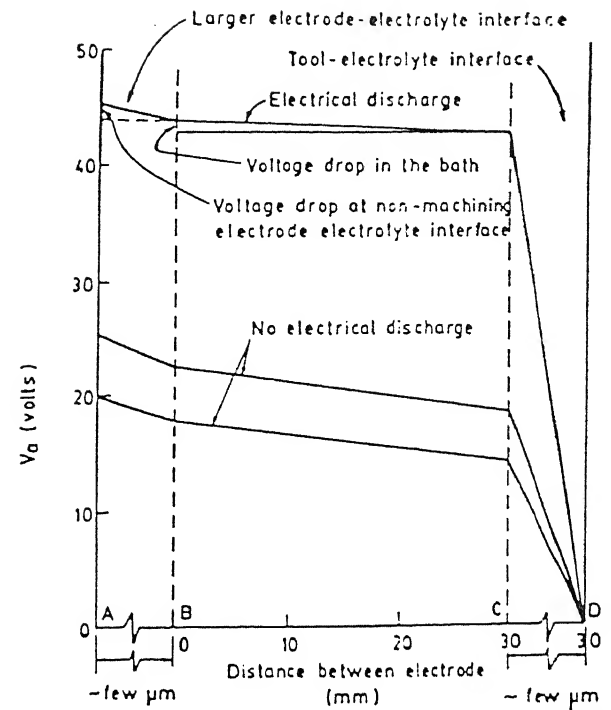
Distribution of voltage drop in an ECDM bath [Electrolyte : NaOH(35%); Tool polarity : -ve ; Power supply : DC] [1]
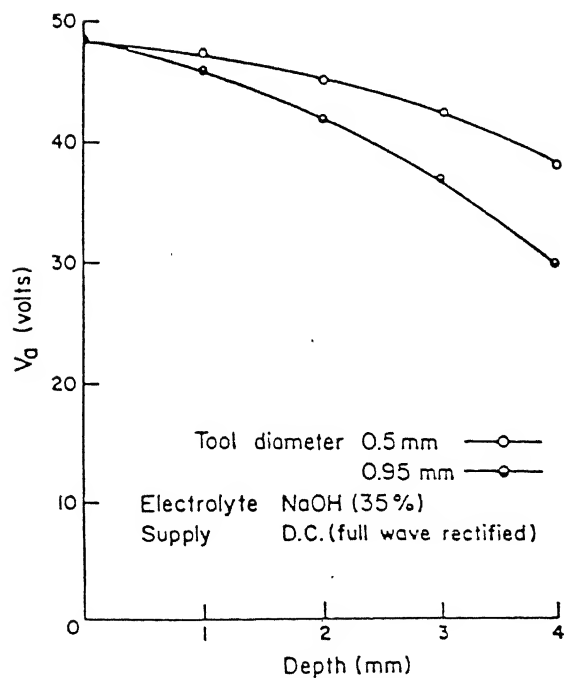
Potential variation along the hole [1]
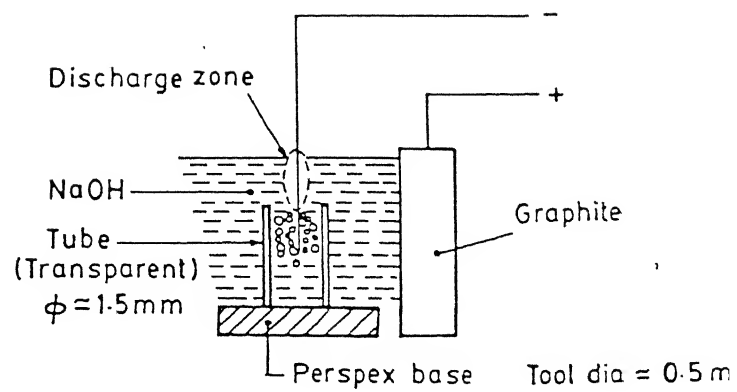
Shifting of the discharge zone [1]

Figure 1.9: Experimental observation of ECD phenomenon [1]

to have no effect on TWR whereas MRR decreases slightly with increase in fiber volume fraction.

Jain et al. [13] did experimental investigations into travelling wire electrochemical spark machining (TW-ECSM) of composites. They reported increase in MRR, toolwear rate (TWR) and overcut with increase in voltage and NaOH electrolyte concentration up to 20 percent. Beyond this concentration it decreases, primarily because the specific conductance decreases beyond 20 percent concentration value. Effect of bubbles was also studied on ECSM process by introducing artificially produced bubbles. It resulted in lower MRR but improved dimensional accuracy.

Tokura et al. [33] reported pit forming by electro chemical discharge process in non-conductive ceramic materials such as ASN, Alumina and MSN. While using 0.5 mm diameter Ni needle and 20% NaOH as electrolyte at 70 volts, the maximum depth of the pit that could be made in the alumina was 85 microns.

Chikamori [7] did grooving on Silicon Nitride ceramic with arc discharge in electrolyte. The depth of groove obtained in 60 minutes machining was about 1.5 mm using $NaNO_3$ solution in water at 165 volts. The tool (Cu) wear rate was below 0.1% by volumetric ratio.

Indrajit Basak [3] conducted experiments on ECD and ECDM. He developed a quantitative model predicting the critical voltage and critical current to initiate the spark. He has also developed a model to predict MRR in ECDM for certain given conditions. It was pointed out that the critical current is a function of equivalent surface area of the tool electrode. He has concluded that electrical discharge takes place due to switching action and not due to dielectric breakdown of the medium,

which is electrolyte. It has also been suggested that for rough machining operations, an inductance should be introduced in the circuit because of which two hundred percent increase in MRR can be achieved.

Y. P. Singh [30] designed and fabricated a Travelling Wire Electro-Chemical Spark Machine and conducted experiments with partially electrically conducting materials like piezoelectric ceramics (PZT) and carbon fiber reinforced epoxy composites. He studied the effect of variation in voltage and electrolyte concentration on MRR and overcut.

Nesarikar et al. [24] carried out TW-ECSM for slicing of kevlar-epoxy composites. Electrolyte conductivity, voltage and specimen thickness were taken as independent parameters while material removal rate, diametral over cut and work piece damage were taken as responses. During their work electrolyte flushing was also tried successfully. The objective was to limit the variation in electrolyte temperature and to remove the debris of workpiece and graphite from the electrolyte tank.

1.6   Objectives and Scope of the Present Work

The literature survey reveals that no attempt has been made on the non contact type of cutting using ECDM process. Furthermore, in earlier research work only solid and stationary tools have been used [1,8,17,33,33,35]. Hence, in order to enhance the capabilities of ECDM process, following main objectives of the present work are envisaged:

- To design and develop a mechanism for controlled feed and rotating tool to conduct orbital drilling operations in the electrically non-conducting materials.

- To explore the possibility of enhancing the limiting penetration depth by using orbital rotating tool, with and without electrolyte flow through it during ECDM.

- To find out the feasibility of using ECDD (drilling) process for borosilicate glass, quartz and alumina.

The secondary objective is to study the effect of tool rotation speed, tool eccentricity and electrolyte flow on the machined hole geometry and its surface integrity.

Chapter 2

EXPERIMENTAL SET-UP AND EXPERIMENTATION

Experiments have been conducted on an experimental electro-chemical discharge drilling machine, specially designed and fabricated for this purpose. The present chapter deals with its design, related instrumentation and experimentation.

2.1 Electro-Chemical Discharge Drilling Machine (ECDDM)

The Electro-Chemical Discharge Drilling Machine has been designed keeping in view the fundamental mechanism of the process and the basic requirements. The drawing of the assembled machine is shown in figure 2.1. The ECDDM can be divided into three distinct subassemblies:

1. Work holding and its feed mechanism (Fig. 2.2)

2. Tool holding and its drive mechanism (Fig. 2.4)

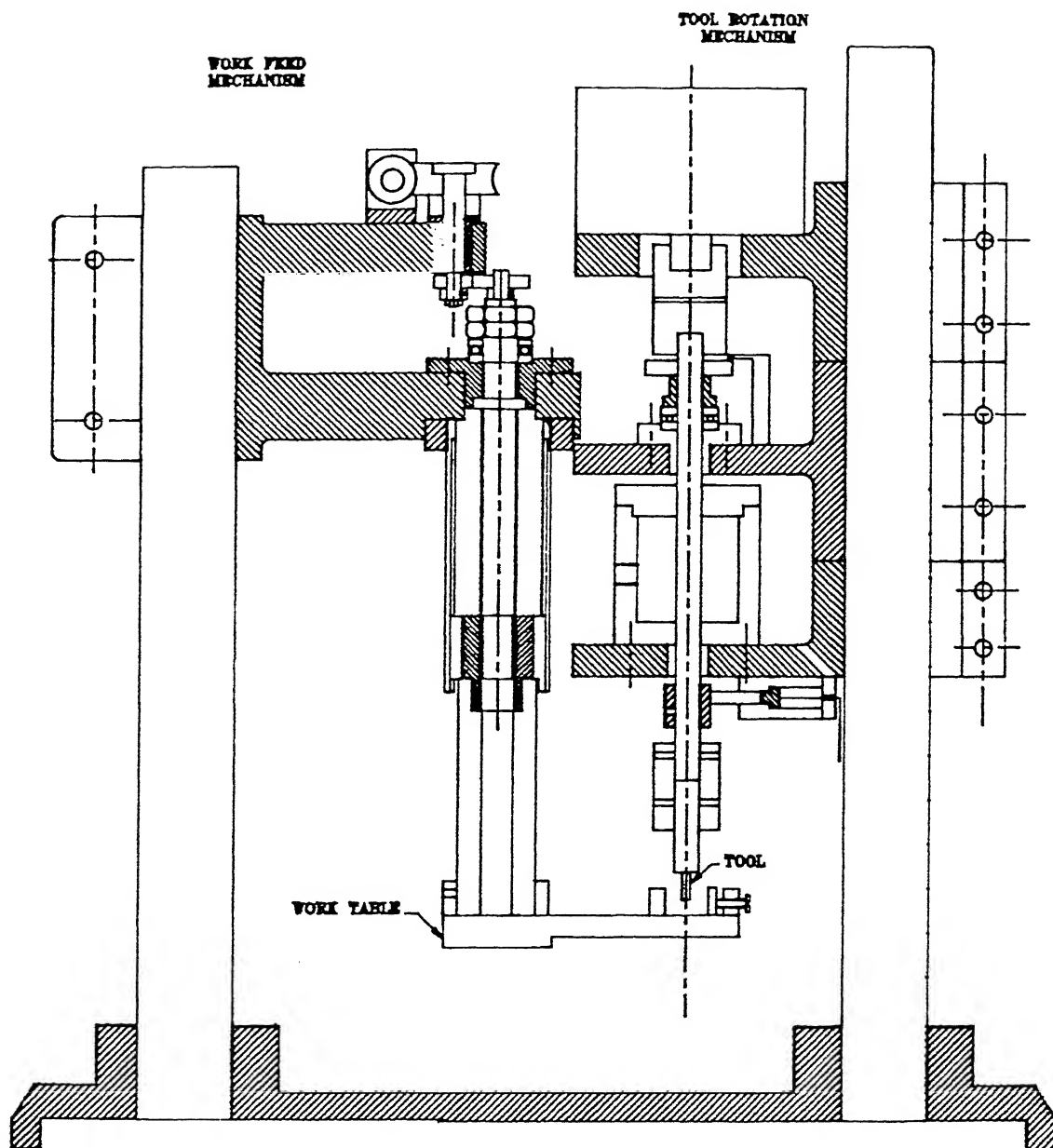3. Electrolyte flow system (Fig. 2.6)

WORK FEED
MECHANISM

TOOL ROTATION
MECHANISM

TOOL

WORK TABLE

Figure 2.1: Electrochemical Discharge Drilling Machine

2.1.1 Work feed and its holding mechanism

The constraint of the feed mechanism was to obtain very low feed rate (2 μm/min)for the machining of ceramics. The minimum feed which can be provided with controller and reduction gear arrangement is 2 μm/min, while the highest feed is 1.2 mm/min. Fig. 2.2 shows the work feed and work holding mechanism. Work piece is held in a vice (1) attached with a worktable (2), both are made up of perspex. This portion of mechanism remains inside the electrolyte during the experimentation. Worktable is attached to a perspex cylinder (3) through a collar (4). Worktable can be adjusted in the XY plane at any angular position, and it can be rigidly clamped with the help of tightening screw (5). This perspex cylinder is thread fastened to a sliding nut (6). The sliding nut is having two key ways and slides inside a brass cylinder (7). Two keys are clamped to the brass nut at 180. The motion to the nut is provided by a SS lead screw (8) having 1.5 mm pitch and getting rotational motion from a stepper motor (not shown in the figure) through reduction arrangement. This stepper motor is fitted on a CI platform (9) which is clamped on a column (10). The height of the CI platform can also be adjusted by sliding it on the column. The column is rigidly fixed with a CI base (11).

For getting a high reduction ratio (40:1), worm (12) and worm wheel (13) reduction is used. Through the gear (14) and pinion (15), further reduction (2:1) is obtained. Worm shaft (16) is coupled to stepper motor shaft through a sleeve coupling (not shown in the figure). Worm is supported on a CI bracket (17) mounted on the CI platform.

A SS pin (18) is used to transmit the motion of worm wheel to the pinion (Z=21). Both worm wheel and pinion are positively mounted on the SS pin. The

1. WORK VICE
2. WORK TABLE
3. PERSPEX CYLINDER
4. COLLAR
5. TIGHTENING SCREW
6. SLIDING NUT
7. BRASS CYLINDER
8. LEAD SCREW
9. PLATFORM
10. COLUMN
11. BASE
12. WORM
13. WORM WHEEL
14. GEAR
15. PNION
16. WORM SHAFT
17. BRACKET
18. PIN
19. BUSH
20. THRUST BEARING
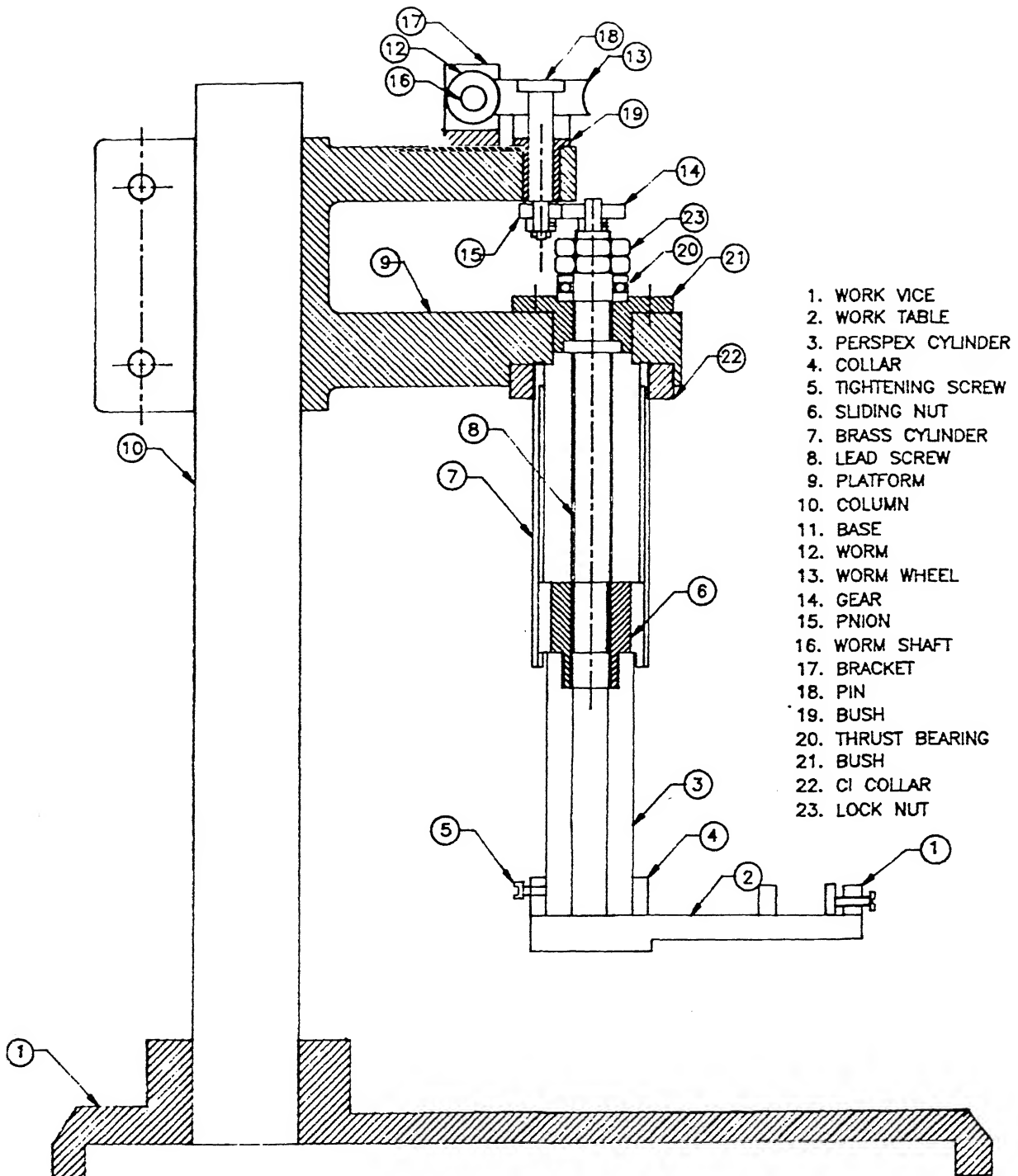21. BUSH
22. CI COLLAR
23. LOCK NUT

Figure 2.2: Work Feed Mechanism

pin is supported on another fork of the CI platform. Brass bush (19) is tightened in the platform in which SS pin rotates. A gear (Z=43)is used for further reduction and engaged with the pinion. The gear is mounted on the lead screw. The entire lead screw subassembly including sliding nut, perspex cylinder and worktable is vertically supported on a thrust bearing (NACHI) (20). The thrust bearing is resting on a brass bush (21) which is screw tightened on the CI platform. The brass cylinder which provides guide to the sliding nut is vertically clamped on the CI platform with the help of CI collar (22). Related part drawings are shown in figure 2.3.

2.1.2 Tool holding and its drive mechanism

The important requirements which were kept in mind while designing the tool rotating mechanism are as follows:

1. True rotation of the tool at the desired speed.

2. Continuous electrical supply during tool rotation.

3. Proper insulation of the tool from the various supports and motor.

4. Through hollow passage for the supply of the electrolyte in the machining zone.

Figure 2.4 shows the tool drive mechanism. The hollow spindle for the supply of electrolyte is made up of SS tube (1), which is rotated by a stepper motor (2). Shaft of the motor is coupled with the SS tube with an insulated claw coupling (3). The motor is supported on a cast iron motor platform (4), which is clamped on a vertical column (5). The insulated coupling and entire spindle tool sub assembly is
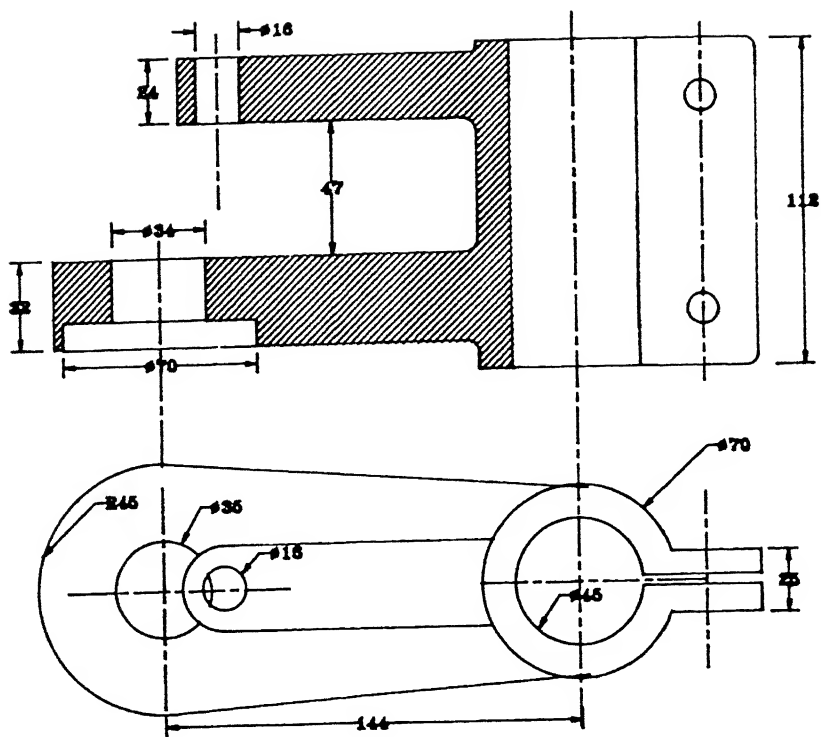
MOTOR STAND
(CI)
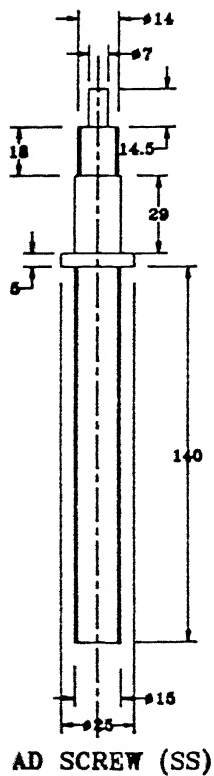
AD SCREW (SS)
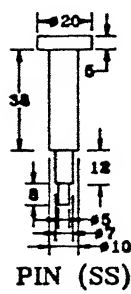
PIN (SS)

CYLINDER
(BRASS)

COLLAR
(BRASS)

Figure 2.3: Contd.

SLIDING NUT
(BRASS)

BUSH
(BRASS)

COLLAR
(BRASS)

WORK VICE (PERSPEX)

CYLINDER (PERSPEX)
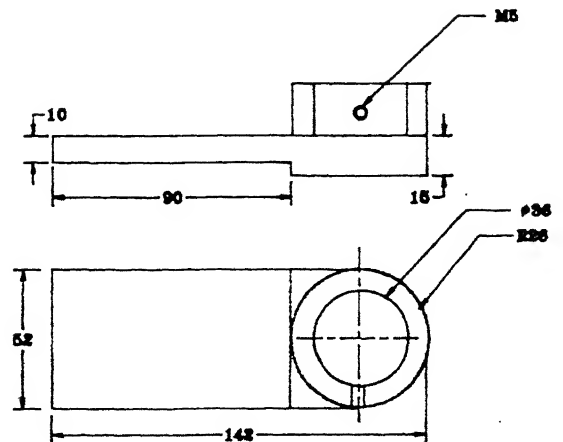
WORK TABLE (PERSPEX)

Figure 2.3: Part drawings of work feed mechanism

vertically supported on a thrust bearing (6) with the help of brass collar (7), which is tightened on the spindle. The thrust bearing is supported on a teflon bush (8), which provide an insulated guide to the spindle. The teflon bush is screw tightened on a CI bearing platform (9).

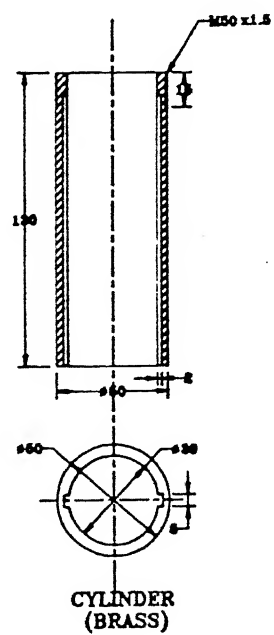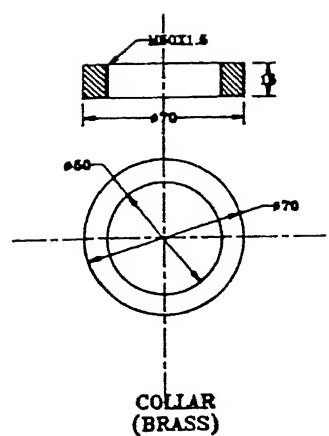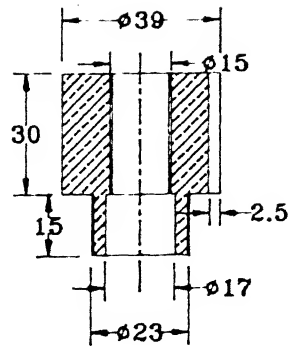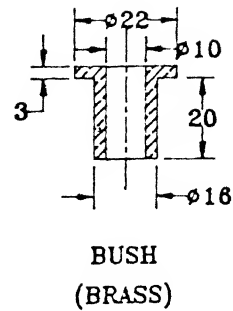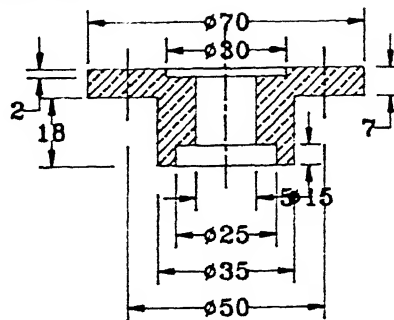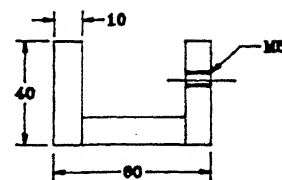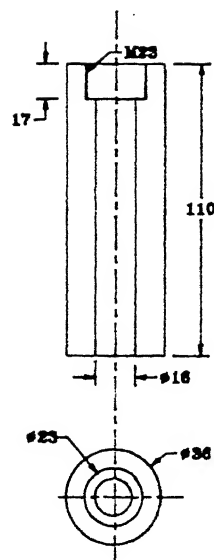The vertical chrome plated column is rigidly supported on a base (10). Three independent cast iron platforms are clamped on the column which can slide on it. Motor is supported on the top platform, thrust bearing on the teflon bush is supported on the intermediate platform and electrolyte chamber is supported on the lower platform (11).

Continuous electrical supply is provided to the tool during the rotation by a carbon brush-slip ring arrangement. Spring loaded carbon brush (12) is kept in a perspex casing (13), which is screw tightened to the lower face of the electrolyte chamber platform. Electrical wire extension (14) is taken from the carbon brush, which can be connected to the desired polarity of the power source. A brass sleeve (15) is tightened on the spindle. Carbon brush is continuously rubbing on this sleeve for providing spark free continuous electrical contact.

Tool (16) is attached to the lower end of the spindle with the help of a brass sleeve (17) in the form of coupler. To get the true rotation of the tool, two grub screws at 180° are provided. Different tool holding arrangements are used as per the requirements of the experimentation. Related part drawings are shown in figure 2.5.

Eccentric rotation to the tool is provided with the help of a special tool holding mechanism as shown in figure 2.5 b. Tool is fixed on a slider which can slide in a slot. Eccentricity for the tool rotation is adjusted with the help of two screws, which

1. SPINDLE
2. STEPPER MOTOR
3. INSULATED CLAW COUPLING
4. MOTOR PLATFORM
5. COLUMN
6. THRUST BEARING
7. COLLAR
8. TEFLON BUSH
9. BEARING PLATFORM
10. BASE
11. ELECTROLYTE CHAMBER PLATFORM
12. CARBON BRUSH
13. BRUSH CASING
14. ELECTRIC CONNECTION
15. SLEEVE
16. TOOL
17. COUPLER
18. ELECTROLYTE CHAMBER
19. MICRO SWITCH
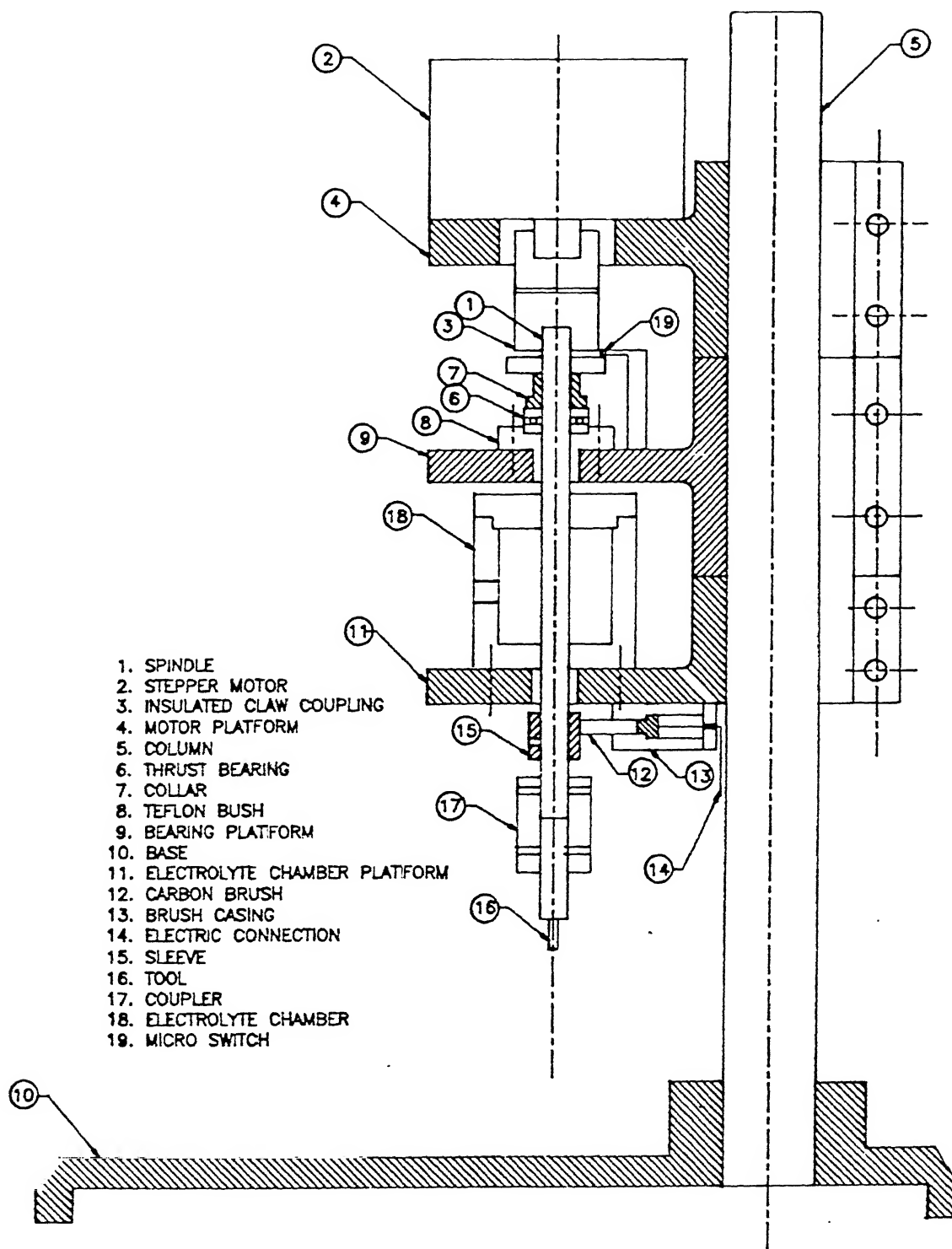
Figure 2.4: Tool Drive Mechanism

BEARING PLATEFORM
(C I)

MOTOR PLATEFORM
(C I)
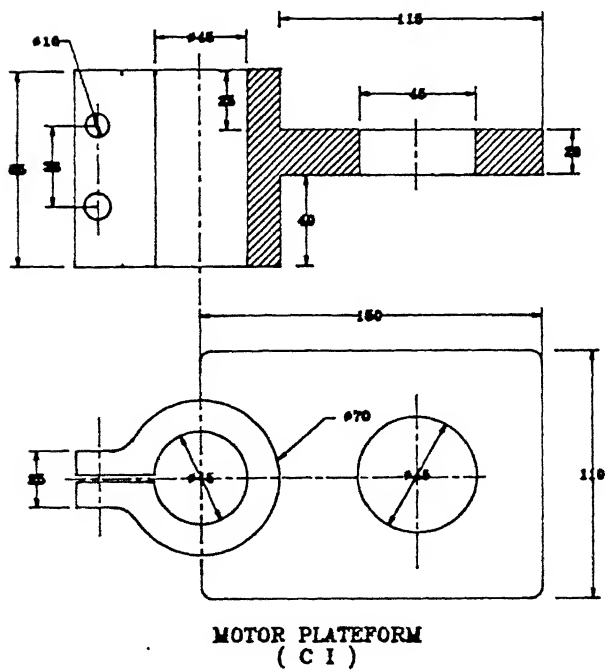
Figure 2.5: Contd.

ELECTROLYTE CHAMBER PLATEFORM
(C I)

1. PERSPEX C
2. PERSPEX C
3. CARBON BR
4. BRASS PUSH
5. SLIP RING

CARBON BRUSH — SLIP RING ASSEMBLY PARTS

Figure 2.5: Cont d

BUSH
(TEFLON)

COLLAR
(BRASS)

ELECTROLYTE CHAMBER
(NYLON)

(a)

Spindle

Slider
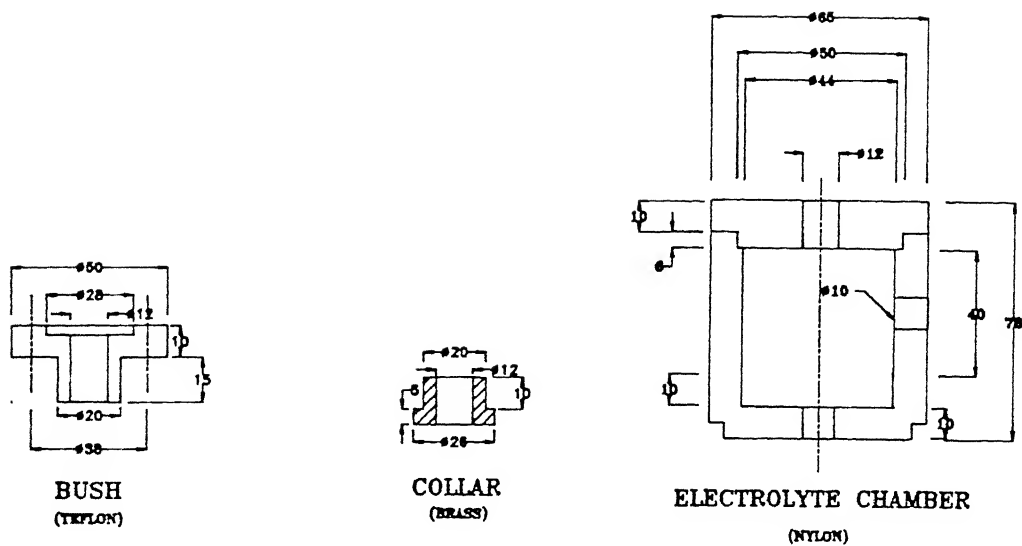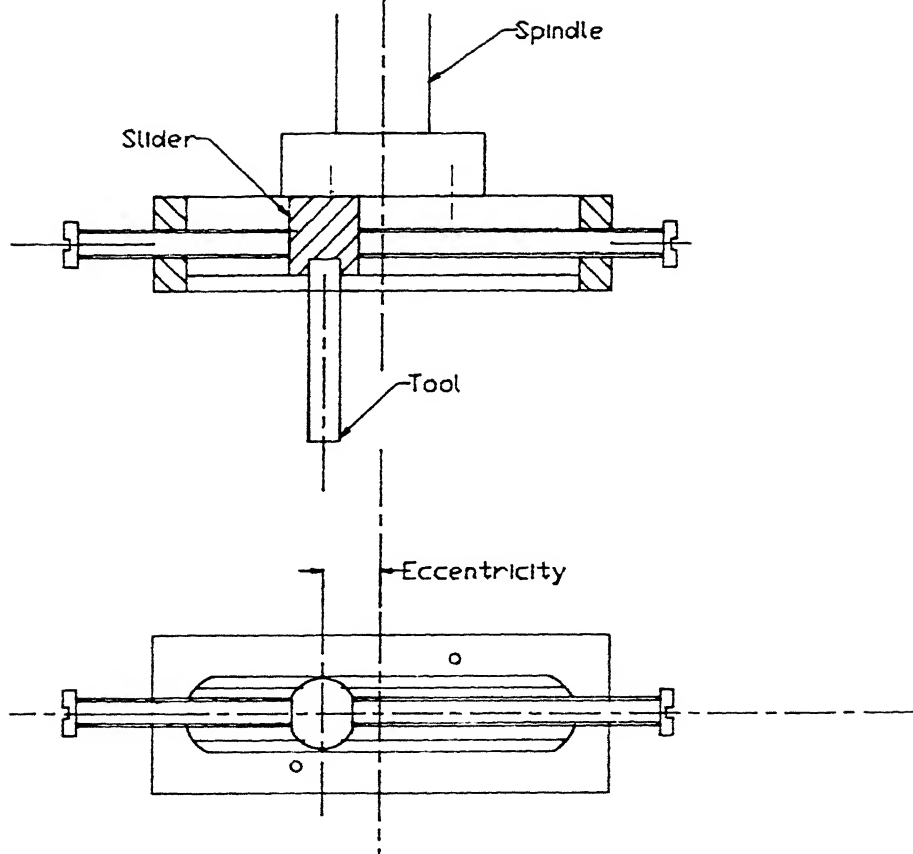
Tool

Eccentricity

(b) Tool holding mechanism with eccentricity

Figure 2.5: Part drawings of tool drive mechanism

hold the slider at a particular location in the slotted slider rest. Spindle is attached to the slider rest with screws through a disc.

2.1.3 Electrolyte flow system

Figure 2.6 shows the electrolyte flow system. Electrolyte flow chamber is used for continuous flow of the electrolyte through the hollow rotating tool. Electrolyte chamber, made up of green nylon is provided with teflon sealing at both the ends to make the leak proof rotational joint. Electrolyte chamber receives electrolyte from an over head tank and supply is regulated with the help of a button valve. Holes are provided in the hollow spindle that passes through the electrolyte chamber. Upper end of the spindle is sealed in order to avoid leakage from the top.

2.2 Electric Power Supply

The constant regulated 220 volts A.C. power was taken from a C.V.T. (constant voltage transformer) through an auto transformer (variac), step down transformer, bridge rectifier and capacitor bank. The output obtained was smooth rectified D.C.

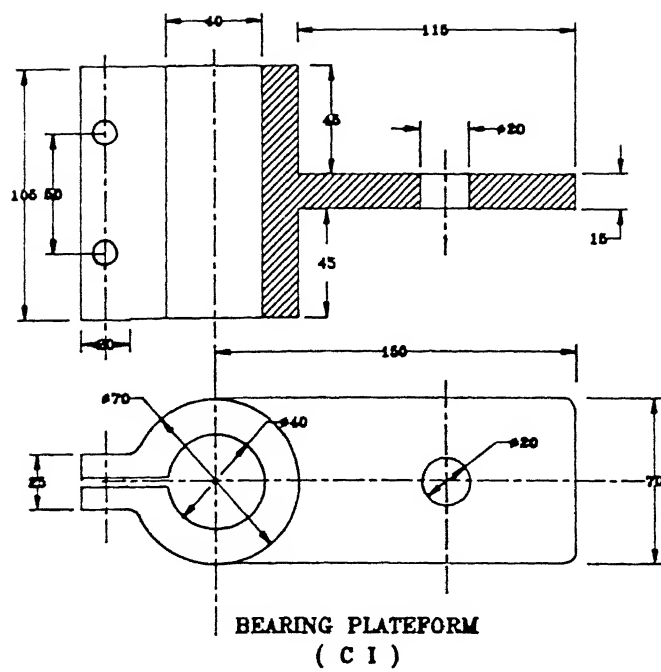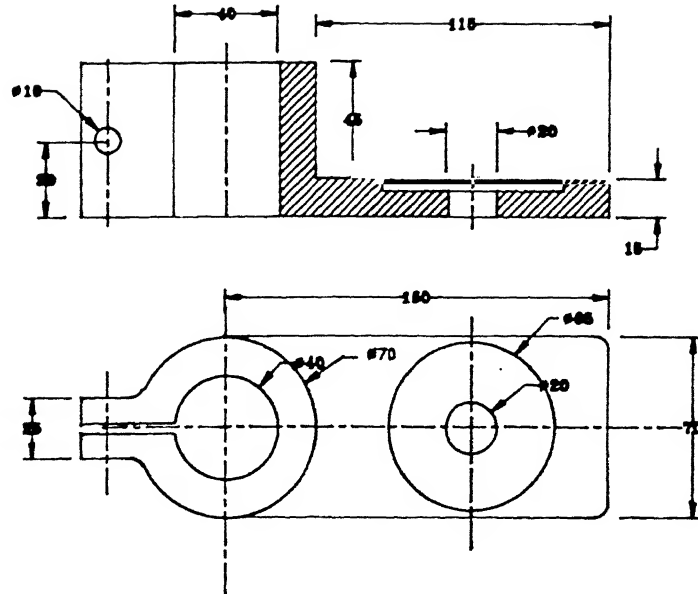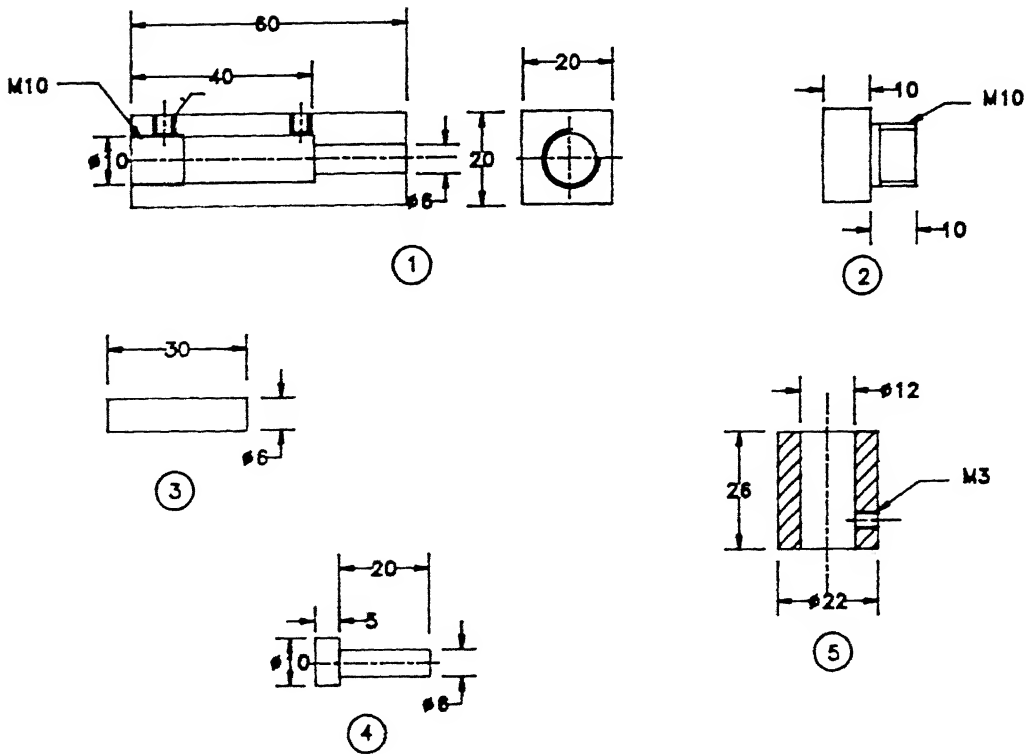Figure 2.7 shows schematic diagram of the electric circuit. A diode bridge (diode specification 2SM70) is used for rectification of A.C. and a bank of capacitors of capacitance 1980 micro-farad and 400 volts is used for filtering the ripples.

2.3 Drives and Instrumentation

Independent stepper motors with the recommended controllers are used as drives to the work feed mechanism and tool rotation mechanism separately. A 12 volt, 20 kg-

Figure 2.6: Electrolyte Flow System

230 V AC

VARIAC

TRANSFORMER

DIODE
BRIDGE

CAPACITOR
BANK

DC OUT
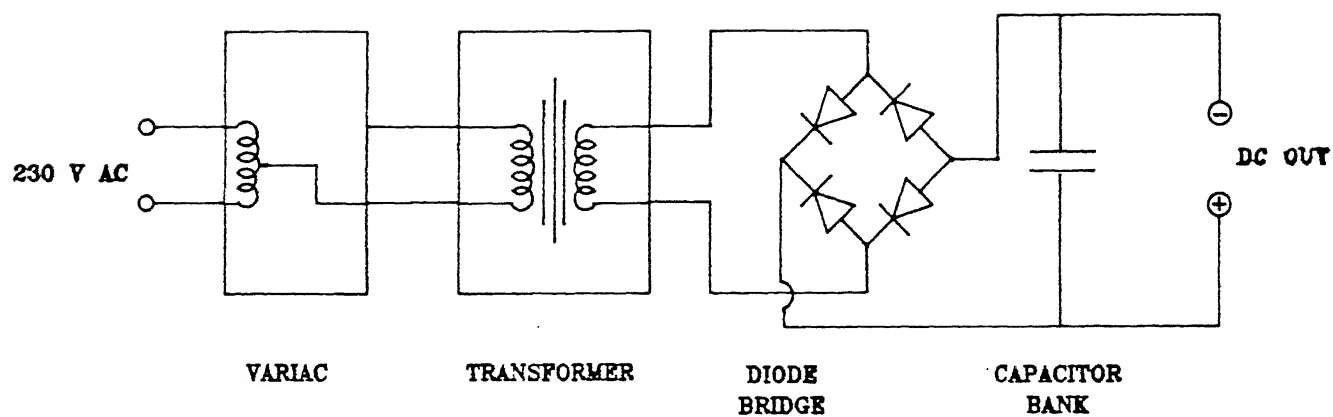
Figure 2.7: Power supply for ECDM set up

cm torque motor is used for work feed mechanism and 12 volt, 7 kg-cm torque motor is used for tool rotation mechanism. Both these motors are controlled separately by two independent 'Unistep' controller.
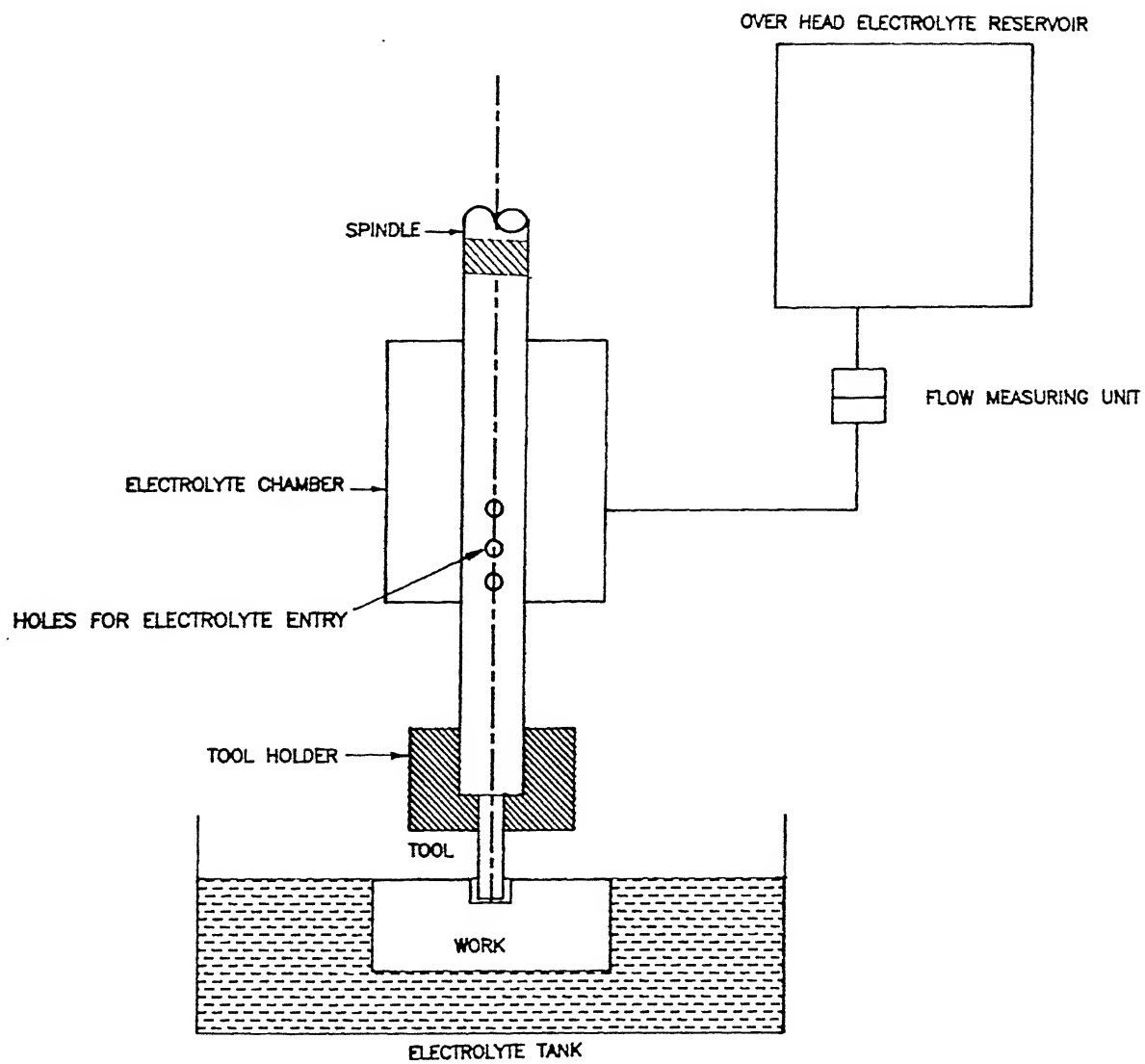
2.4 Tool Work Contact Sensing Mechanism

In the present machining process, work material is non conducting in the nature. Machining is possible because work is placed in close vicinity of the sparking zone. For efficient machining, the ideal condition is that there should always an appropriate gap between the work and tool, so that the hydrogen and vapour bubbles are available for sparking to take place inthat region. Researchers [1,3,8,17,32,33,35] have worked with gravity feed tool thus, continuous contact was maintained during the machining. This may also be a factor contributing for achieving very low machining depth.

In EDM, due to requirement of the process nearly a constant gap is maintained during the process with the help of servo control feeding system, which is possible to obtain by pulse monitoring. While machining the non conducting materials such sensing and feeding system can not be used because pulse in ECDM is not the function of the gap.

Figure 2.8 shows a schematic diagram of the mechanical type sensor designed for sensing the contact between work and tool. When contact occurs between work and tool due to the higher feed rate as compared to machining rate, upward force lifts the tool with spindle. Provision is made for this movement of the spindle by providing a sufficient clearance at the insulated claw coupling (3 in Fig.2.4). A brass disc (2) is tightened with the spindle which operates a micro switch (1).

Electrical signal is obtained as soon as micro switch operztes. Feed motion direction is reserved manually in order to generate required clearance and to over come the play of microswitch.

2.5 Electrolyte

It was revealed from the literature survey that most of the work has been done with alkaline electrolytes such as NaOH and KOH. To compare the present results with those obtained by the previous researchers, the experiments have been conducted using NaOH as electrolyte.

Fresh NaOH solution was prepared and allowed to cool down to the room temperature in still air, since the dilution of NaOH is an exothermic reaction. Solution was kept in closed container in order to minimise the evaporation losses, which may change the concentration of the solution. Conductivity of the electrolyte solution was checked using a digital conductivity meter (CENTUTY DD 101) and kept within $\pm 3\%$ of the desired value before starting any experiment. This was acchived by adding fresh solution or water depending on the requirements. Temperature of the solution was also maintained within $\pm 1^\circ C$ of the desired value before the start of any trial.

2.6 Work Material

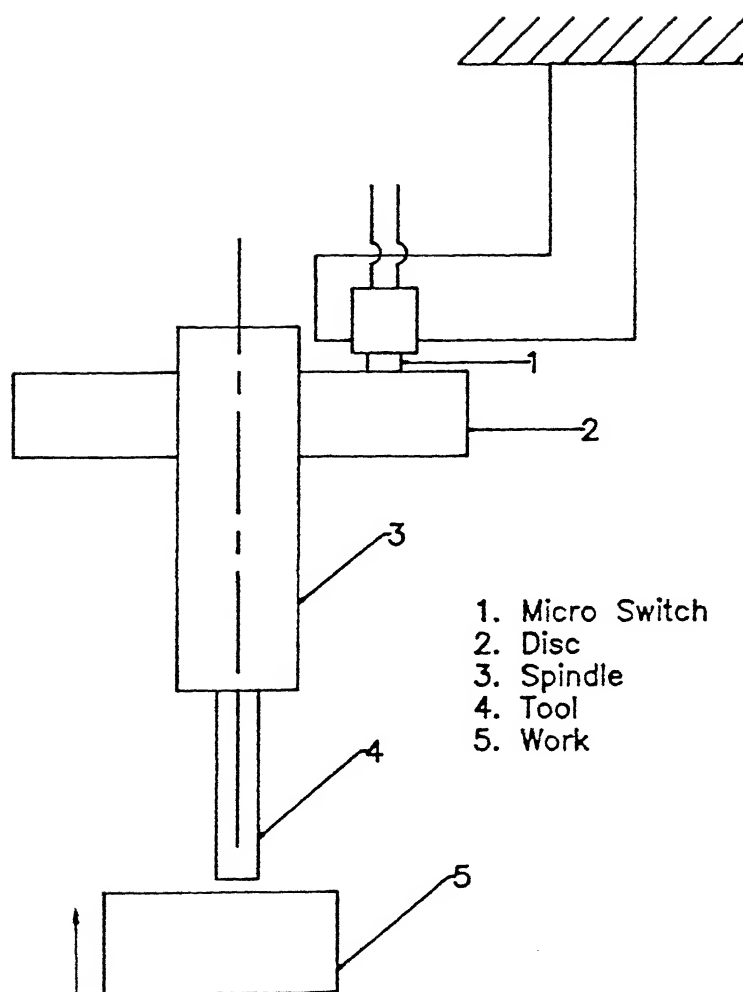Various electrically non-conducting materials, as given below, have been used as work materials :

1. Micro Switch
2. Disc
3. Spindle
4. Tool
5. Work

Figure 2.8: Tool Work Contact Sensing Mechanism

2.6.1 Borosilicate Glass

Borosilicate glasses constitute a large proportion of industrial glasses (laboratory glasses, neutral glasses for pharmacy, glasses for electronics, micro porous glasses etc.). The glass specimens used for the experimental work were supplied by Corning Corporation under the trade name of Pyrex.

Thin walled vessels of borosilicate glass can withstand instantaneous quenching in cold water from temperature $195°C$. Physical and chenical properties of borosilicate glass are given in the appendix A.

2.6.2 Quartz (Silica Glass)

Compared with other glassy substances, silica glass exhibits the lowest thermal expansion, high resistance to thermal shocks, high chemical durability, high hardness, high transmission in the ultra violet, visible and infrared parts of the spectrum and last but not least a high softening temperature. Because of these properties silica glass is an ideal technological and industrial material. The clear silica glass which is used for the experimental purpose contains approximately $99.9\% SiO_2$. Physical and chenical properties of borosilicate glass are given in the appendix B.

Thin walled vessels of silica glass can withstand instantaneous quenching in cold water from temperature $800° - 1000°C$ and rapid cooling down from $1300°C$ in a stream of cold air.

2.6.3 Sintered Alumina

Sintered alumina is much less expensive to make as compare to crystalline alumina. It has been widely used at high temperature and in diverse applications such

as refractories, lamp tubes, grinding pebbles, polishing compounds, electronic substances, spark plugs, laboratory ware etc. The alumina samples which were used for experimental work have been sintered at $1550°C$. Physical and chenical properties of borosilicate glass are given in the appendix C.

2.7 Experimentation

A graphite plate is made as anode in the ECDDM set up and placed approximately at a distance of 8 mm from the tool end. Potential is applied across the graphite plate (anode) and tool (cathode). A conductivity meter is used to record specific conductance of the electrolyte and a thermometer to measure its temperature.

The specimen is properly placed in the work vice and vice is tightened. Feed decision was a major problem in ECDM. Work piece is moved for feeding purpose, so as to minimize the effect of shifting of discharge zone (sec.1.4), when tool is fed in drilling operation. Mechanical type work tool contact sensor (sec.2.4), is used for this purpose. Machining is started with a constant gap (100 μm) and higher feed rate is provided then the estimated penetration rate obtained from the preliminary experiments. Due to higher feed, force is exerted on the tool, which lifts the spindle by small distance (150 μm). This movement actuates the micro switch and a signal (glowing of the bulb) is obtained. Feed is reversed manually immediately. Machining continues and spindle moves downward with the rate equal to the sum of reversal work feed and tool penetration rate. When the switch is completely relieved, which is indicated by the electrical signal, feed is resumed. For all the experiments feed is kept constant. Real time contact sensing remained a major problem throughout the experimentation. Test conditions used during the experimentation are given in
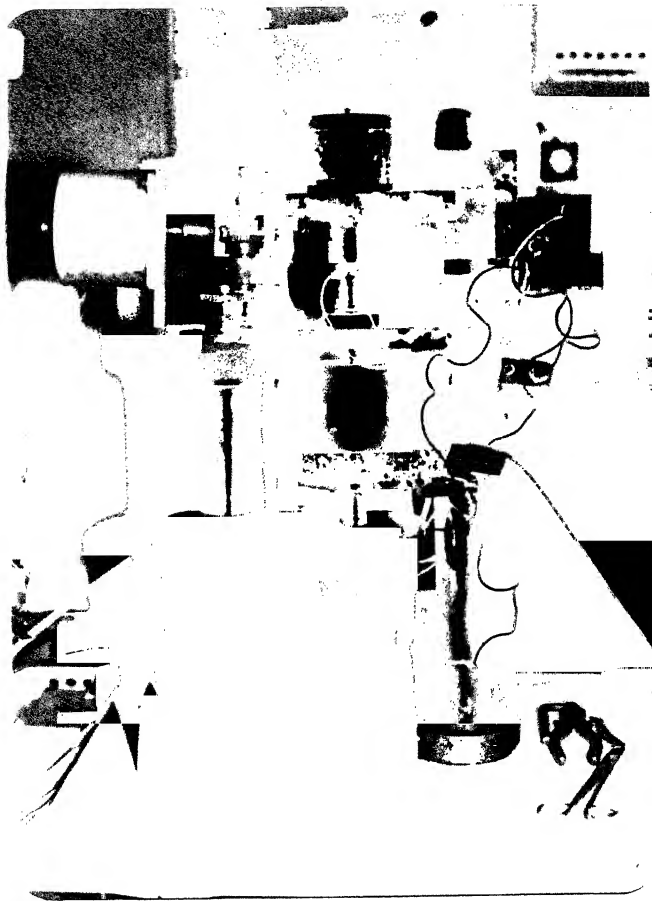
(a) Electrochemical Discharge Drilling Machine
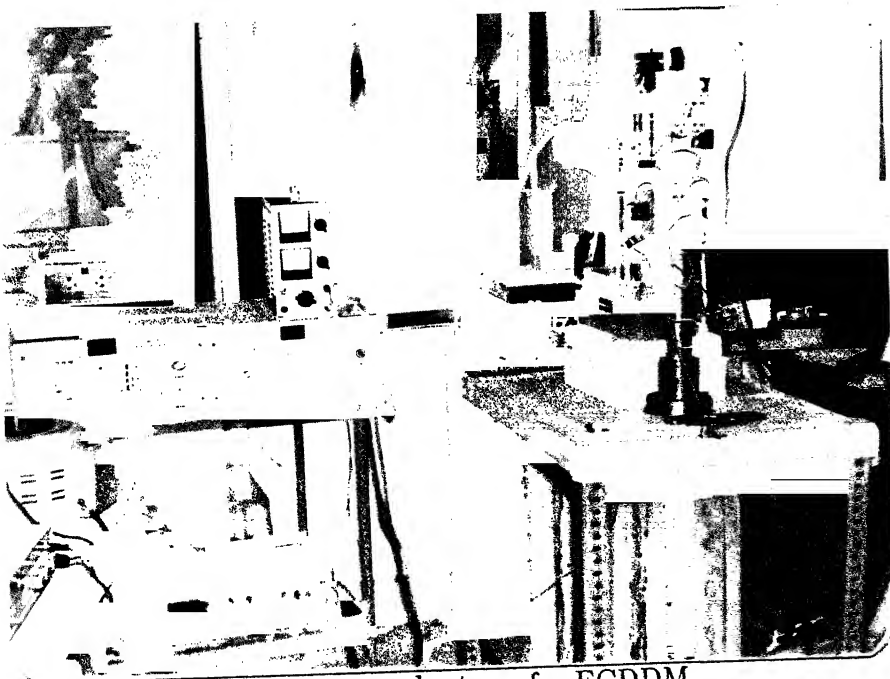
(b) Experimental set up for ECDDM

Figure 2.9

Electrolyte	$20\% NaOH$
Electrolyte temperature	$24° \pm 1°C$
Conductivity	300 ± 3 mmho/cm
Feed rate	1.05 mm/min (Glasses)
	50.25 μ m/min (Alumina)
Tool tip depth in electrolyte	3 mm
Tool diameter	1.68 mm
Speed range	0 - 80 rpm
Flow rate	0 - 100 cc/min

Table 2.1: Test conditions

table 2.1.

The specimen is rinsed with tap water thoroughly to remove the layer of electrolyte. Then, it is dried by heating to expel any water particle which might be present particularly in the machined blind holes. The amount of material removal was determined by the the weight difference method. A mechanical micro balance (MLW, VEB, Analytic) of range 0 - 100 grams and with an accuracy of 0.01 mg was used for this purpose. The average penetration depth and diameteral over cut from the are taken on shadow graph .

Chapter 3

RESULTS AND DISCUSSION

3.1 Introduction

Tool kinematics plays an important role in ECDM process. Almost all researchers [1,3,8,17,32,33,35], have worked with gravity feed and non-rotational type of tool (i e stationary tool) electrode for drilling operation. During this course of study different combinations of tool kinematics and electrolyte flow were tried to study their effects on the performance of ECDM process. In this chapter, results are reported while using stationary tool, rotating tool, eccentrically rotating tool and electrolyte flow through hollow rotating tool. In each case, feed to the work was given as discussed in sec. 2.4. Grapher package is used for plotting various graphs.

Geometrical parameters of the machined hole such as taper and circularity error are also disused. Results of surface integrity, studied with the help of scanning electron microscope, of the machined surface are also presented and discussed. Effects of various controllable parameters on the responses are given below:

3.2   Effect of Machining Time

In ECDM machining rate is not constant with time. As the tool penetrates in side the work surface, machining rate goes down and it reaches almost zero value. For the given machining conditions, the specified work material can be machined only up to a certain depth known as "limiting depth". This characteristic of ECDM has been studied by various previous researchers [1,3,8,32,33,35]. In the present study, attempts have been made, with the help of various tool kinematics, to increase the limiting depth, without sacrificing the quality of the machined surface.

3.2.1   Machining with stationary and rotational tool

The experiments using stationary tools have been conducted to generate the base data for comparing the results obtained by using different tool kinematics. It is evident from the figures 3.1 and 3.2 that variation in the machine depth and material removal with machining time show almost the same trend in both the cases i.e. while using stationary tool as well as rotational tool. However, total amount of machined depth and material removed during the use of rotational tool is more as compared to stationary tool. Following explanation is hypothesized for such behaviour:

Due to rotation of the tool some agitation in electrolyte is created, because of that some used electrolyte may be scavenged out from the machined zone and replased by the fresh one hence, machined depth is increased.

3.2.2   Machining with eccentric tool

Figures 3.3 (for borosilicate glass) and 3.4 (for quartz) show the effects of machining time on machined depth and machining rate while the tool is rotated with different
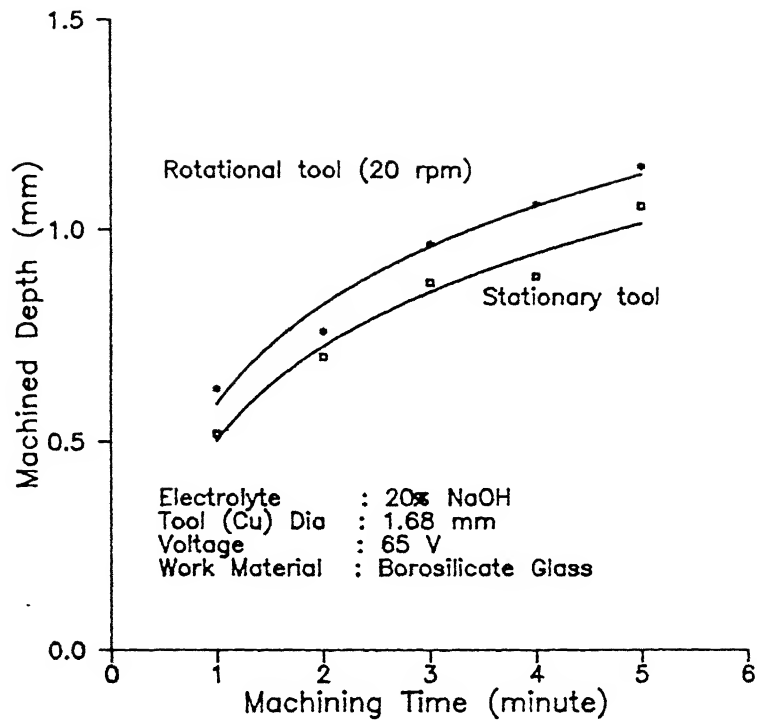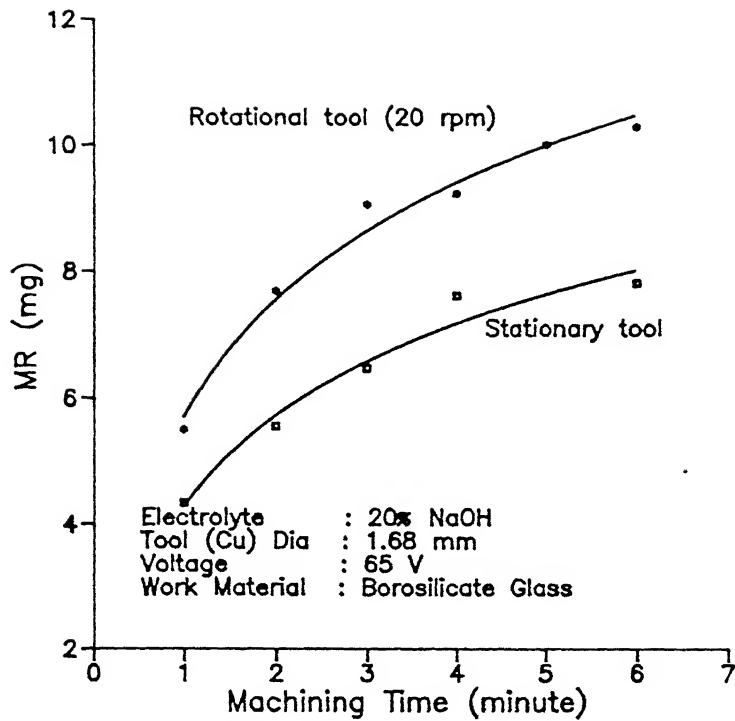
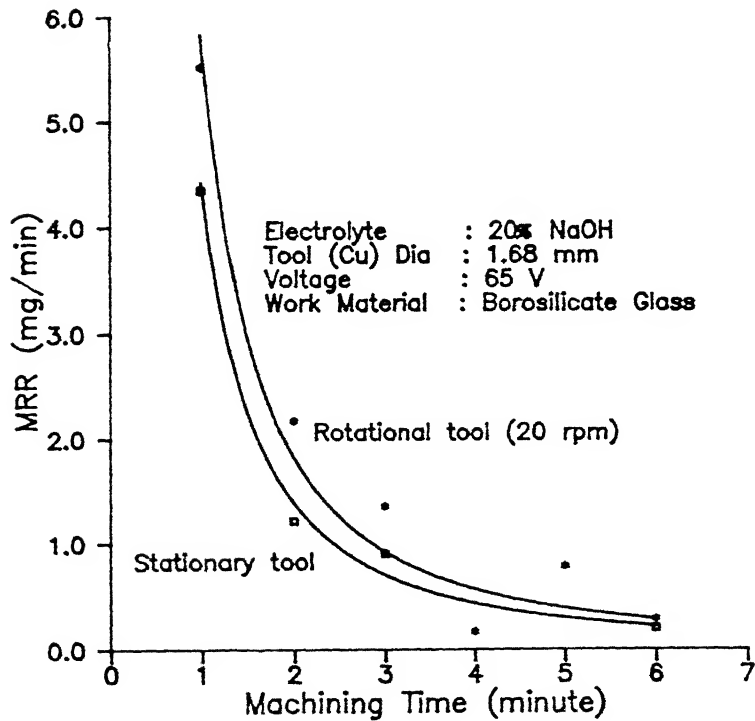(a) Effect of machining time on machined depth.
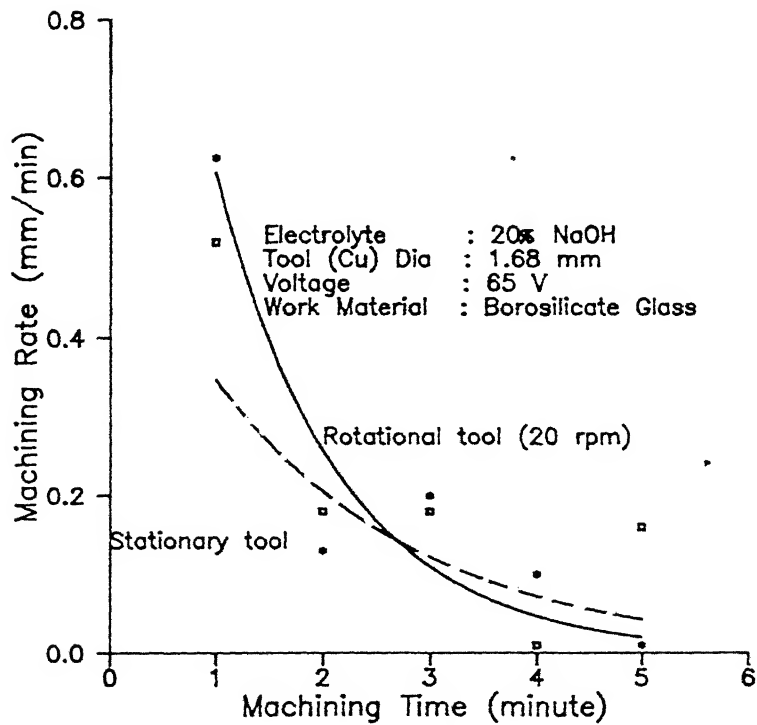
(b) Effect of machining time on machining rate.

Figure 3.1

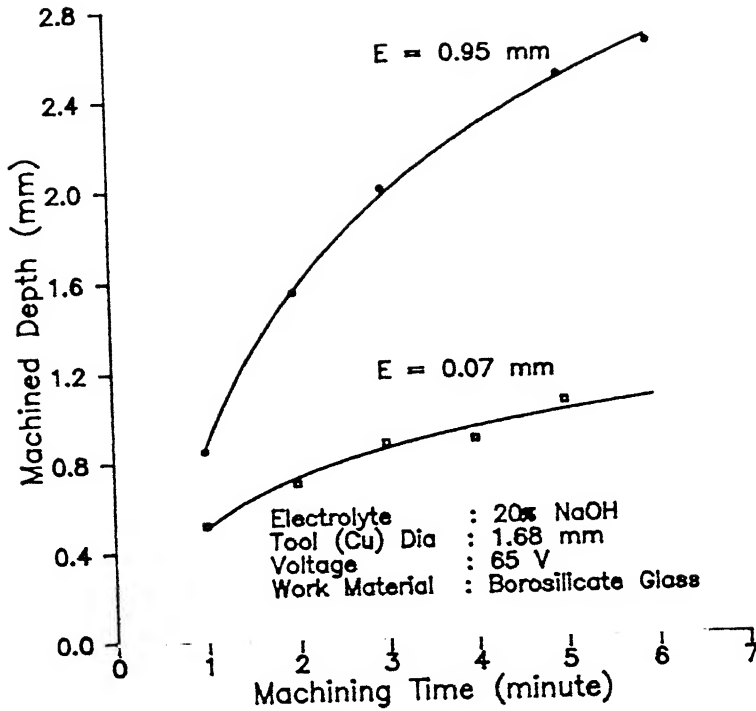(a) Effect of machining time on material removal

(b) Effect of machining time on material removal rate

eccentricities. Figure 3.3 (b) indicates that when a tool with very small eccentricity is used, machining rate becomes negligible after a short period of time as compare to the case with high eccentricity. In case of tool with higher eccentricity (approximately equal to the tool radius), machining continuous and a through hole in a 3 mm thick borosilicate glass tube is possible in 8 to 9 minutes, at 65 V while 20% NaOH solution is used as electrolyte.

The improvement in the process performance can be explained with the help of figure 3.5. At the increased eccentricity more fresh electrolyte is available in the machining zone, which helps in reducing the concentration of contamination due to bubbles and debris. Availability of fresh electrolyte in the machined zone, ensures the required potential difference for discharge to take place between the tool and the electrolyte. Thus, discharge continues in the machining zone even for the higher machined depth.

## 3.3   Effect of Tool Rotational Speed

Figure 3.6 shows the effect of tool rotational speed (revolution per minute - rpm) on machined depth for borosilicate glass and quartz. The rotational speed of tool v/s machined depth characteristic can be divided into two distinct regions for the purpose of explanation of the results. In the region I, the agitation in the electrolyte due to rotation of the tool induces scavenging effect, hence, penetration depth increases with the tool speed. In the region II, the speed of rotation is high enough to play a dominant role in destablization of sparking which results in lower machined depth. It is clear from the experimental observations that machined depth and material removal in case of quartz is always lower than borosilicate glass, which may

(a) Effect of machining time on machined depth using different eccentricities
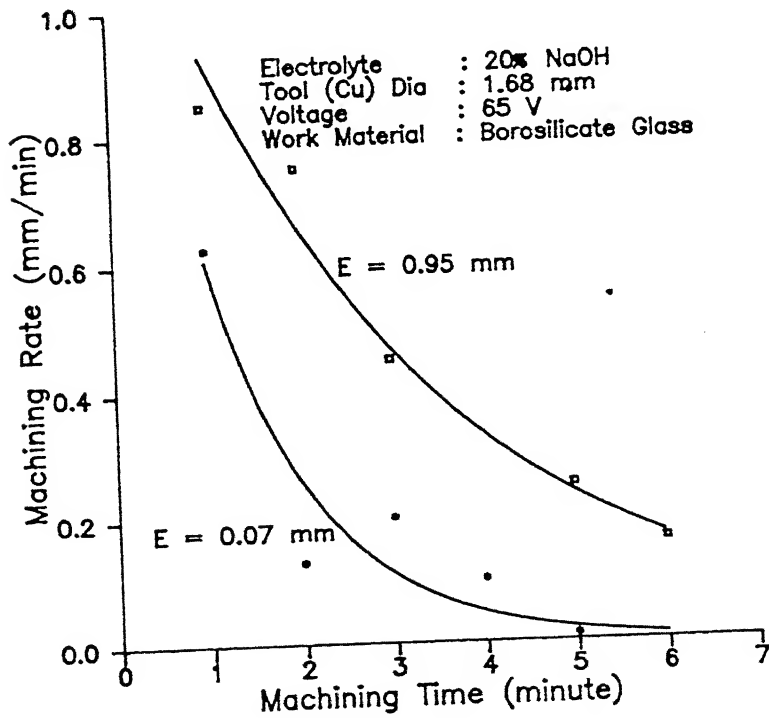
(b) Effect of machining time on material removal using different eccentricities
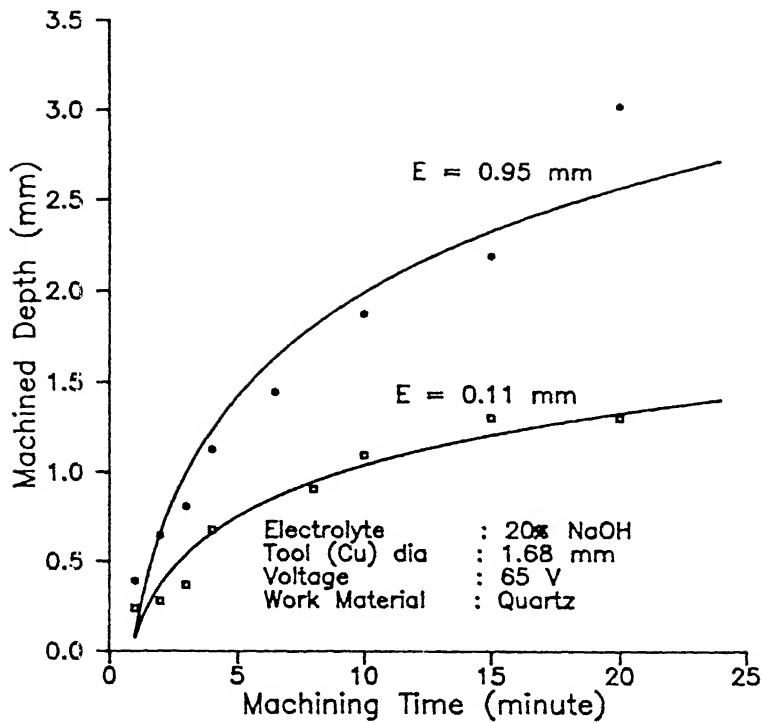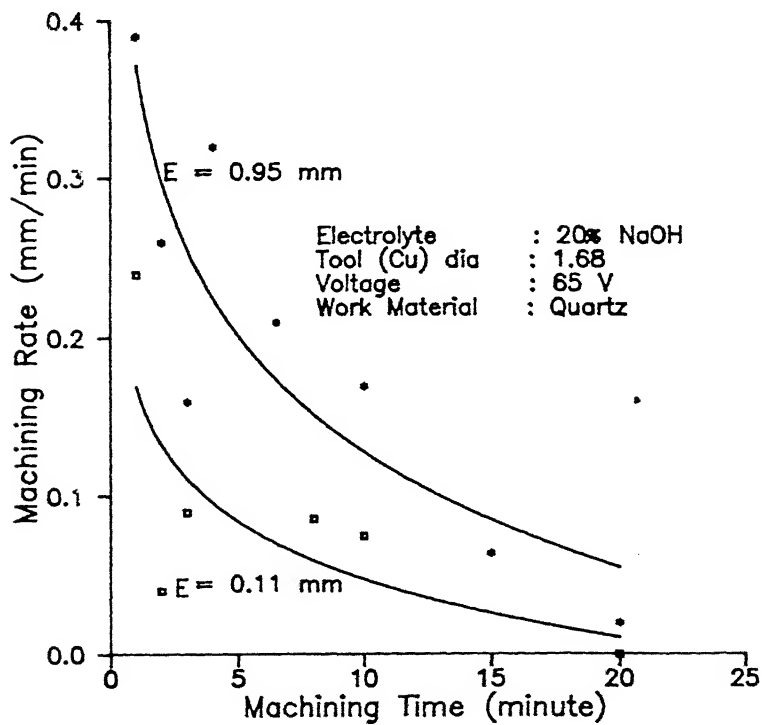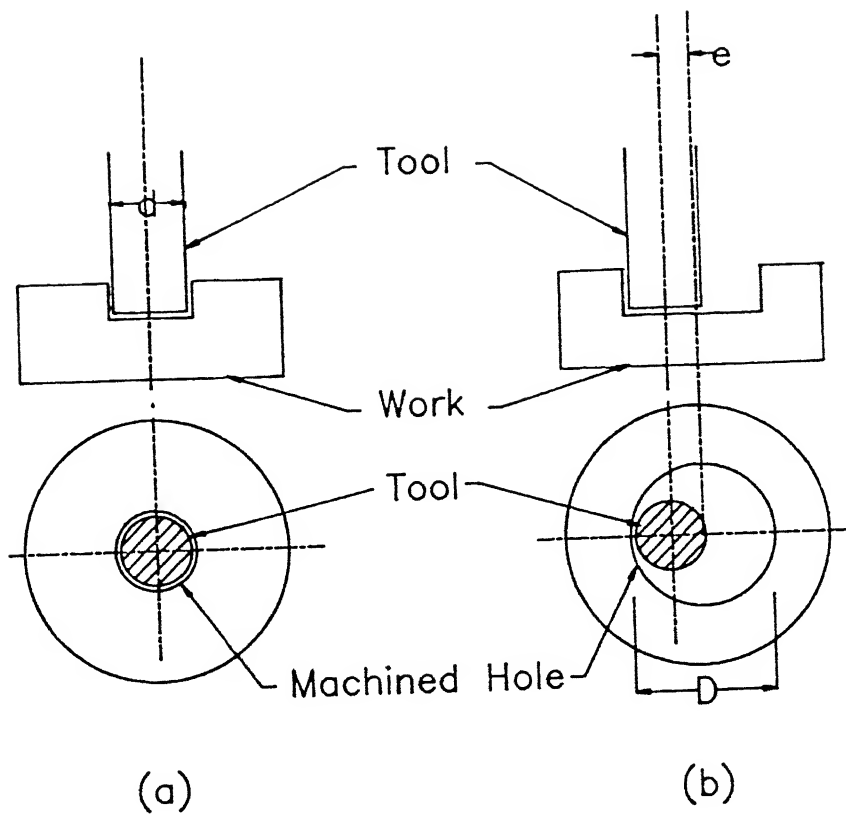
(a) Effect of machining time on machined depth using different eccentricities

(b) Effect of machining time on material removal using different eccentricities

(a) Machining without eccentricity

(b) Machining with eccentric tool

Figure 3.5

be due to its high softening point.

3.4 Effect of Electrolyte Flow

Figure 3.7 shows the effect of electrolyte flow rate on the machined depth during machining of borosilicate glass and quartz using ECDM process. Electrolyte is allowed to flow through a hollow tool which is a hypodermic needle. Both the curves in figure 3.7 indicate that with the increase in electrolyte flow rate, the penetration depth first increases slightly up to a certain value of flow rate, and then after attaining maxima, it starts decreasing. The nature of the electrolyte flow rate v/s machined depth characteristic can be once again explained with the help of flushing and discharge destablization phenomena.

At the low flow rate, flushing effect helps in improving the process performance. After attaining the maxima, further increase in the flow rate starts extinguishing some of the sparks, this resuls in reduced input energy for machining. As a result, machined depth is reduced.

3.5 Effect of Tool Eccentricity

Limited depth of penetration achievable during ECDM is one of the major limitation of the process. Because of this the process has not yet become industrially viable. As already explained in sec. 1.4 [1], the presence of bubbles and debris, in the machined zone, are mainly responsible for limiting depth. Further, rotation of the tool and flow of the electrolyte have been employed to improve the process performance. However, it has been found (Figs. 3.6 & 3.7) that in both the cases, the maxima is
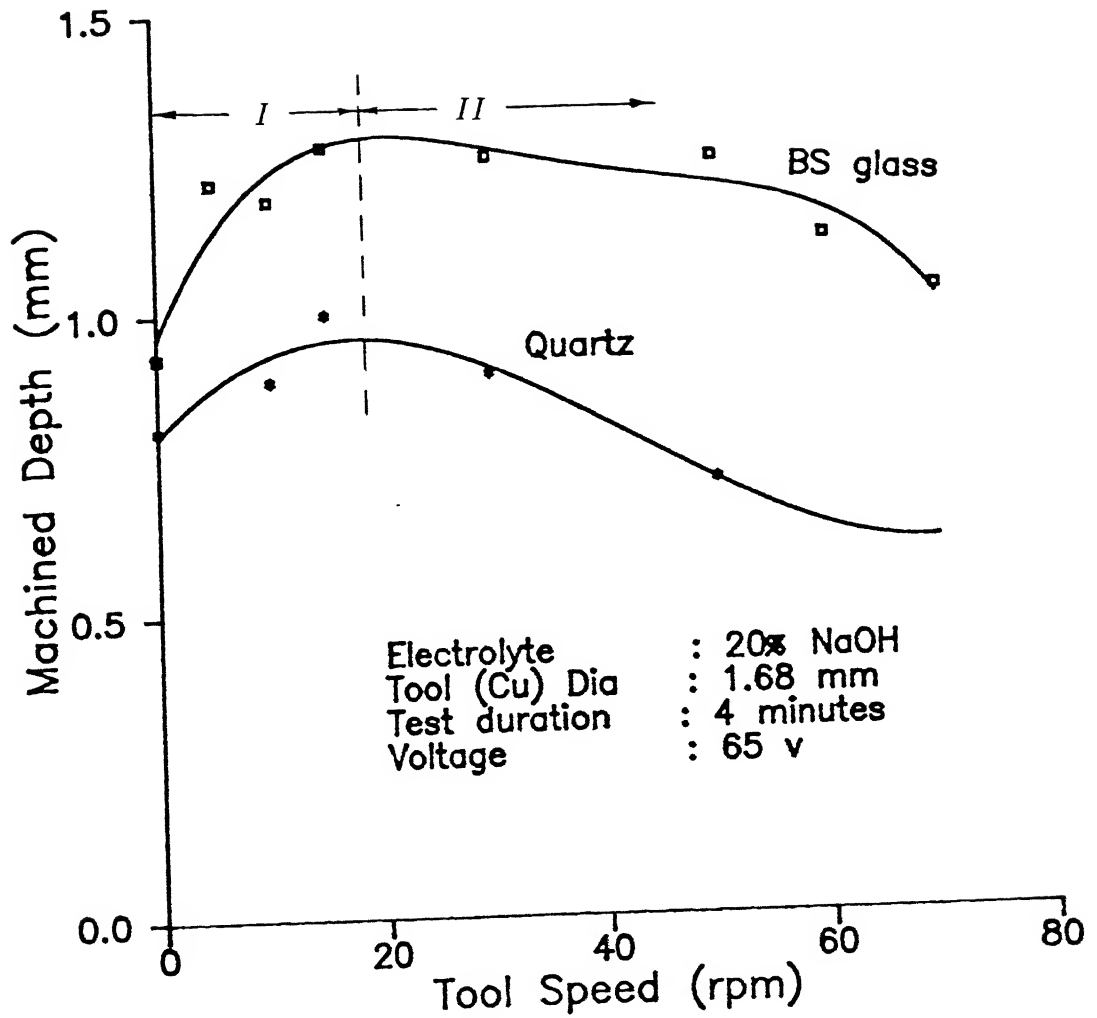
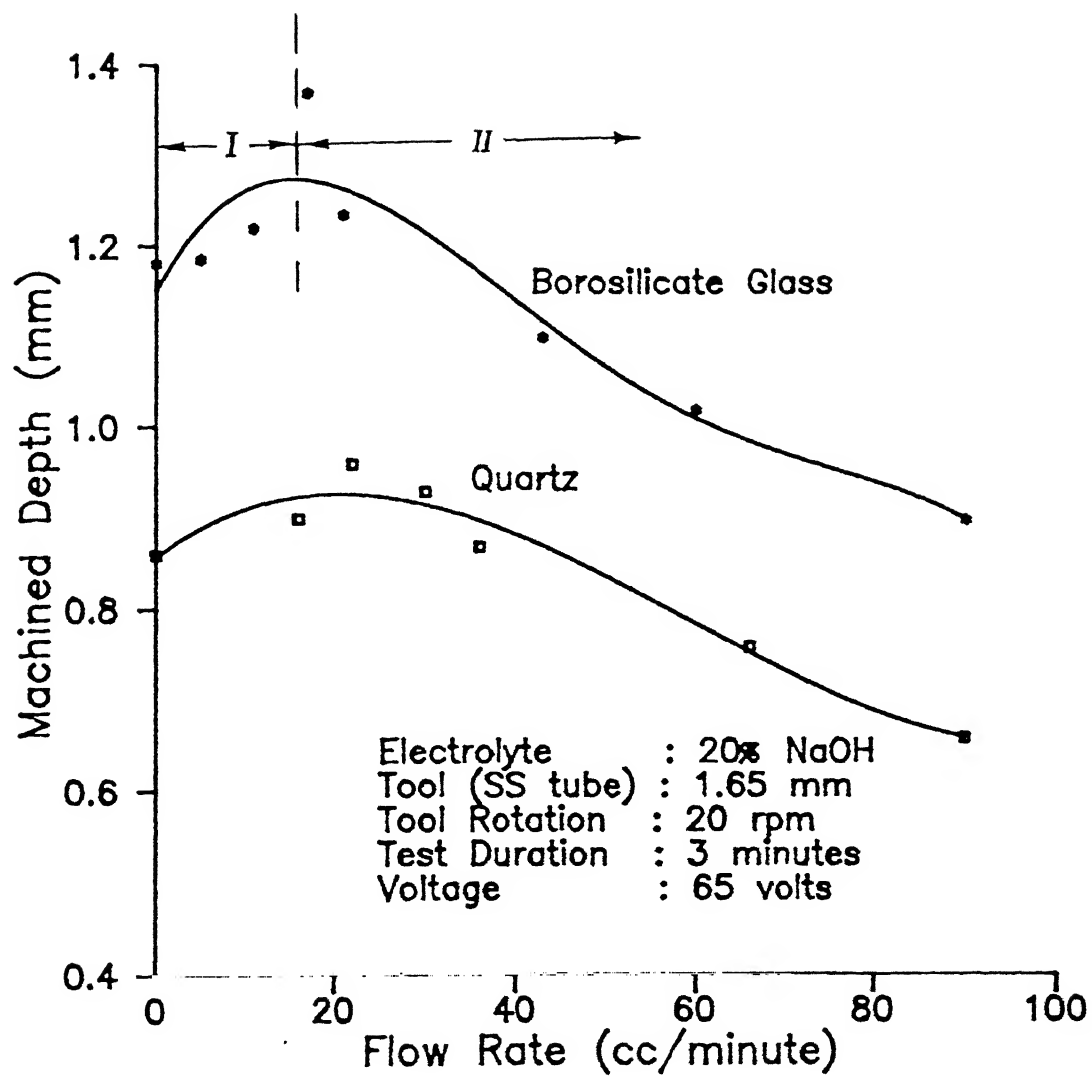Figure 3.6: Effect of tool rotational speed on machined depth

Figure 3.7: Effect of electrolyte flow rate on machined depth

attained at their low values. Beyond these values, any further increase in speed or electrolyte flow rate would adversely affect the process performance.

Figure 3.8 shows the relationship between the tool eccentricity and the machined depth for borosilicate glass and quartz as work materials. It is evident from the given figure that the machined depth increases with the increase in eccentricity. This trend continues till the eccentricity attains the value approximately equal to the tool radius. With further increase in eccentricity, the machined depth starts decreasing. In the first part of the curve (Zone *I*) in figure 3.8 the eccentricity helps in two ways:

- Diameter of the hole (D) in the work is larger as compare to the tool diameter (d). It reduces the concentration of bubbles and debris as compare to the case when the eccentricity is zero (Fig. 3.5)

- Rotating tool at certain eccentricity (e) provides far better scavenging effect than with zero eccentricity (Fig. 3.5).

When the eccentricity is of the order of tool radius, complete sweep cut is possible. However, figure 3.8 shows that eccentricity (e_{opt}) corresponding to the maximum machined depth is slightly higher than the tool radius ($\frac{d}{2}$).

$$e_{opt} > \frac{d}{2} \qquad (3.1)$$

This may be because of overcut which permits sweeping cut situation, even for a little bit higher value of eccentricity.

Diameter (D) of the machined hole in work is given by:
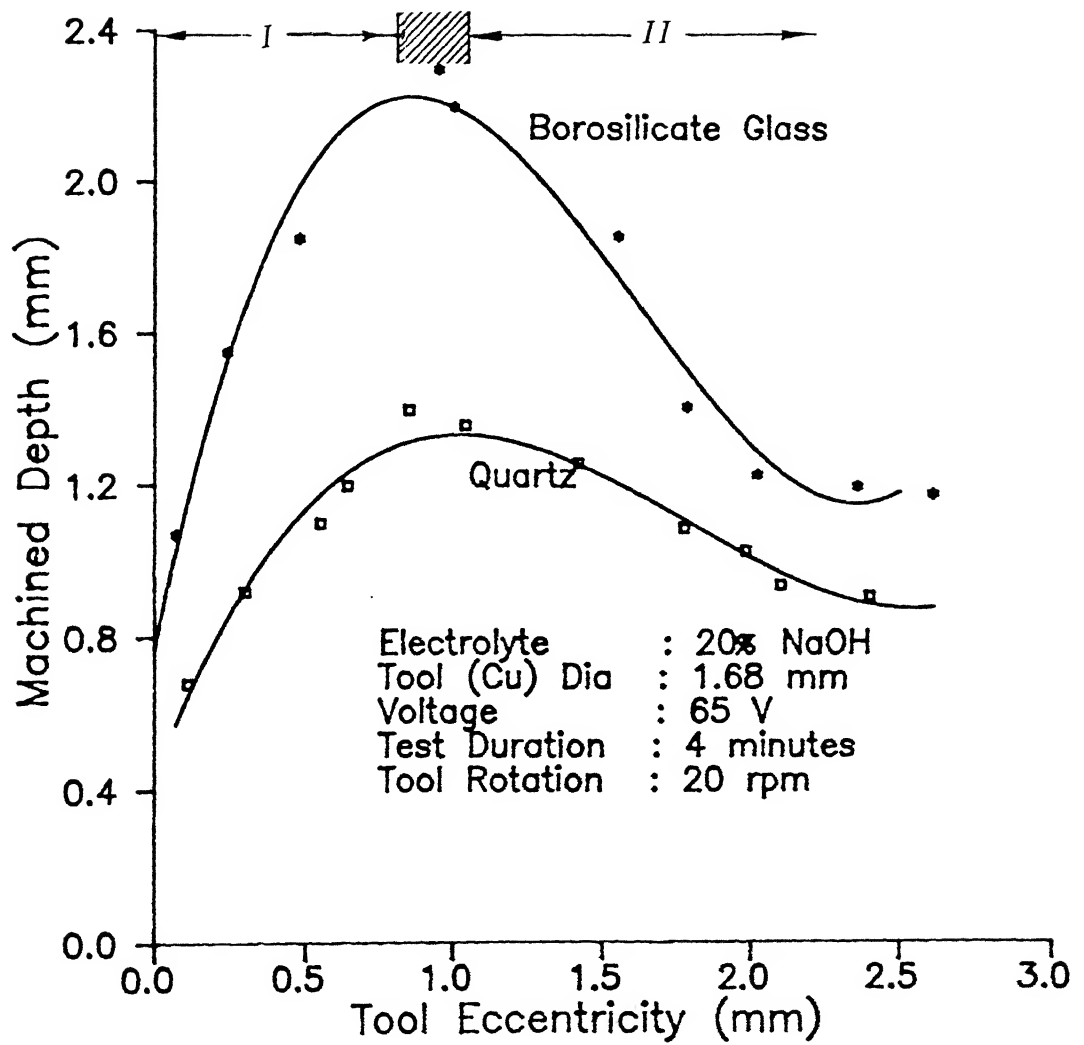
$$D = 2e + d + O_d \qquad (3.2)$$

Figure 3.8: Effect of tool eccentricity on machined depth

where, O_d is diameteral overcut

As the eccentricity is further increased, the sweeping situation is crossed and trepanning cut is acquired (zone II in Fig. 3.8). It reduces the availability of fresh electrolyte thus, reduced machining rate is observed. However, in the transition zone (shown hatched in Fig. 3.8) it can be either sweeping cut or trepanning. During trepanning, material is not removed from the core of the hole as opposed to removing the entire volume of the hole in case of sweeping cut. Therefore, trepanning is always a faster method for generating through holes as compared to sweeping cut. However, for producing blind holes (with sweeping cut) using eccentric tool optimum diameter of the tool (d_{opt}) for generating a hole of diameter (D) is given by:

$$d_{opt} = D/2 - O_d\xi \qquad (3.3)$$

where ξ is a constant depending on the work material

Diameteral overcut (O_d) in ECDM is a function of applied voltage (V), electrolyte type (E), its temperature (T) and concentration (C), chemical reactivity of work material at higher temperature with electrolyte (R), melting temperature (T_m) and evaporation temperature (T_e) of the work material.

$$O_d = f(V, E, T, C, R, T_m, T_e) \qquad (3.4)$$

3.6 Study of Geometrical Parameters of the Machined Surface

Geometrical parameters such as taper and circularity error of ECD drilled are studied and compared in holes machined in borosilicate glass and quartz with different machining configurations, keeping other parameters constant as given in table 3.1.

Applied voltage	$65V$
Electrolyte	$20\% NaOH$
Tool dia	1.68 mm
Test duration	4 minutes

Table 3.1: Test conditions

Figure 3.9 shows the representation used for indicating taperness and circularity error. Shadowgrphs of the various holes machined under above mentioned test conditions with different configuration and work materials are given in figure 3.10.

3.6.1 Taper angle

Taper angles of electro-chemical discharge drilled (ECDD) holes for different machining conditions using borosilicate glass and quartz as work materials are shown in table 3.2. Values of these angles were calculated from the profiles of holes (Fig. 3.10).

Maximum taper angle is observed when gravity feed and stationary tool is used. Use of rotational tool slightly improves the geometry. This improvement is because of more uniform machining due to rotation. Taper angle remains almost same in the speed range from 5 - 50 rpm. Eccentric rotation of the tool and flow of electrolyte through the tool further reduces the taper angle. Lower values of taper angles are always observed with quartz as compared to borosilicate glass because of its higher thermal conductivity which helped in more uniform distribution of heat.

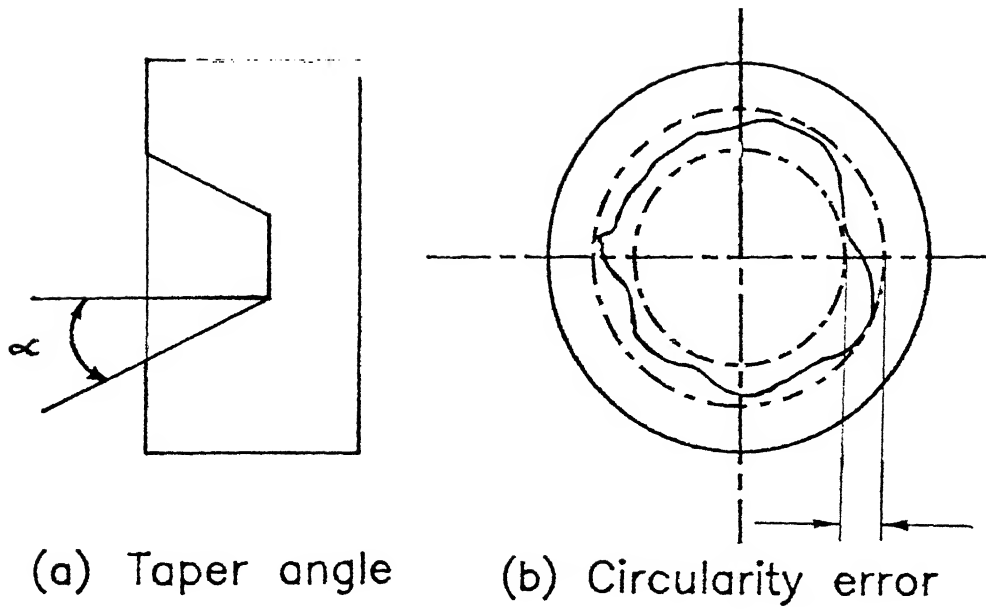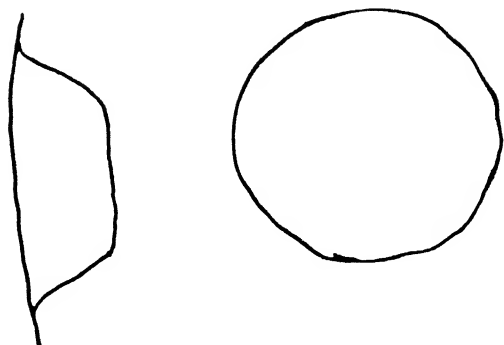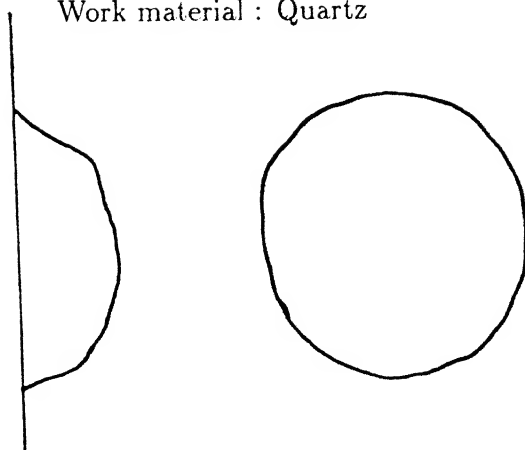(a) Taper angle   (b) Circularity error

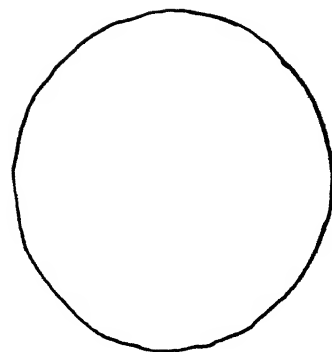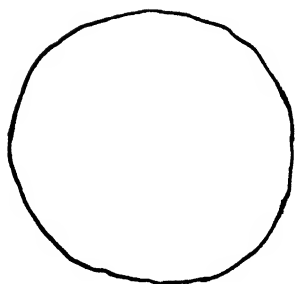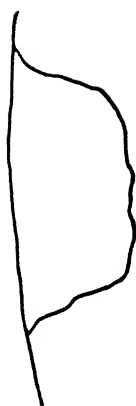Figure 3.9: (a) Representation of taperness (b)Representation of circularity error

Work material : Borosilicate glass

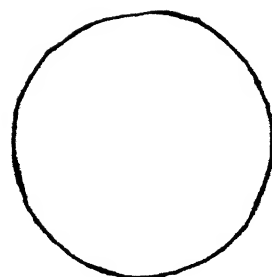Work material : Quartz

Machining with solid stationary tool.

Machining with solid rotating tool.(20 rpm)

1 mm
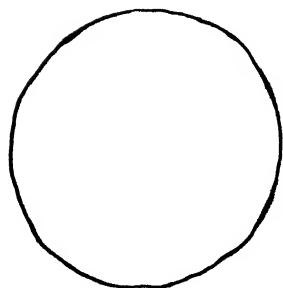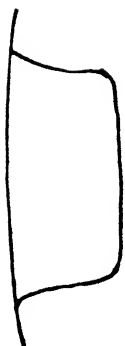
Machining with electrolyte flow through hollow rotating tool (20 rpm)

Applied voltage	65V
Electrolyte	20%$NaOH$
Tool dia	1.68 mm
Test duration	4 minutes

Test conditions

Work material : Quartz

k material : Borosilicate glass
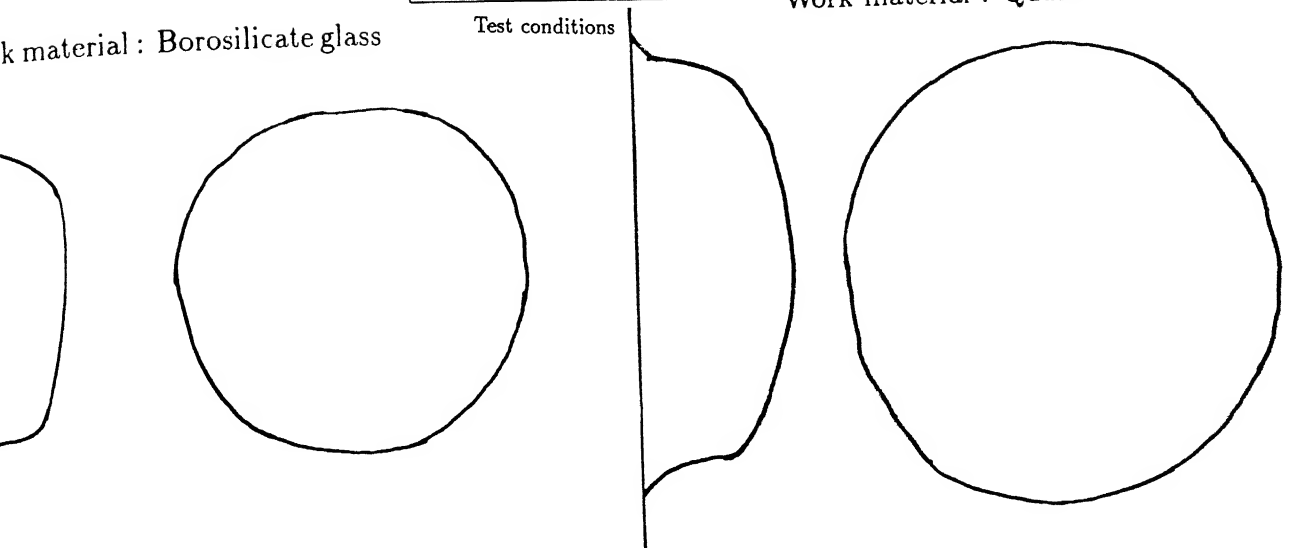
Machining with solid eccentrically rotating tool (20 rpm)

1 mm

Work material : Alumina

Applied voltage	90 V
Electrolyte	20%$NaOH$
Tool dia	1.68 mm
Test duration	15 minutes
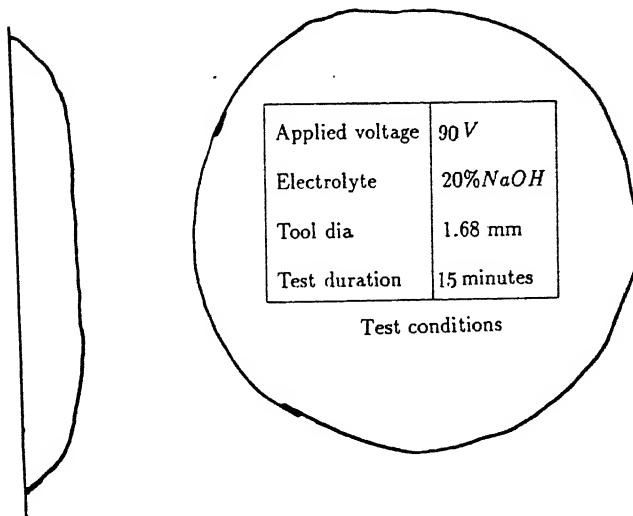
Test conditions

Machining with solid eccentrically rotating tool (20 rpm)

of machined holes under different machining configuration

Machining configuration	Borosilicate glass	Quartz
Stationary tool	31.26°	24.6°
Rotational tool (20 rpm)	23.63°	20.56°
Eccentric tool (20 rpm)	22.24°	17.35°
Electrolyte flow through rotational tool (20 rpm)	20.22°	14.84°

Table 3.2: Taper angles of ECD machined holes with different machining configurations

3.6.2 Circularity error

Circularity errors for different machining configurations (Fig. 3.10) have been shown in table 3.3. Best circularity is observed when electrolyte flow through the rotational tool is used with quartz as work material.

Since cylindrical shaped borosilicate glass tube was used for experimental work, error in circularity for the same could not be studied (elliptical shape is viewed on shadowgraph for a circular hole due to curvature on the surface).

3.7 Surface Integrity of the Machined Surface

3.7.1 Thermally damaged region

Figure 3.11(1) and locally enlarged view in figure 3.11(2) show the thermally damaged zone all around the machined hole in borosilicate glass. SEM photographs show that the thermally damaged region is of the order of 150 microns. For the convenience of analysis this region can be divided into three distinct zones shown in

Machining configuration	Quartz
Stationary tool	300 μm
Rotational tool (20 rpm)	200 μm
Eccentric tool (20 rpm)	300 μm
Electrolyte flow through rotational tool (20 rpm)	100 μm

Table 3.3: Circularity error of ECD machined holes with different machining configurations

figure 3.11(2), namely, heat affected zone intermediate zone and unaffected parent material. Nature of the presence of the intermediate zone can be explained on the basis of existence of high temperature gradient and simultaneous quenching effect. This also resulted in the formation of cracks in this zone. Less severe cracks in this zone are observed in case of quartz, may be due its high thermal conductivity (Fig. 3.11(9,10,11)).

3.7.2 Machined surface appearance

Figures 3.11(3,4,5) (solid rotating tool at 20 rpm) and figures 3.11(6,7,8) (hypodermic needle as tool with flow of electrolyte through it) show the resolidified debris at the bottom surface of the blind hole. These debris are also observed on the wall of the machined surface (Fig. 3.11(12,13)). Thus it can be inferred that the mechanism basically responsible for material removal is thermal phenomenon. It is evident from the SEM photographs (Fig. 1.11(5)) that the global appendages are molten material, which is expelled randomly during the discharge and later solidified on the
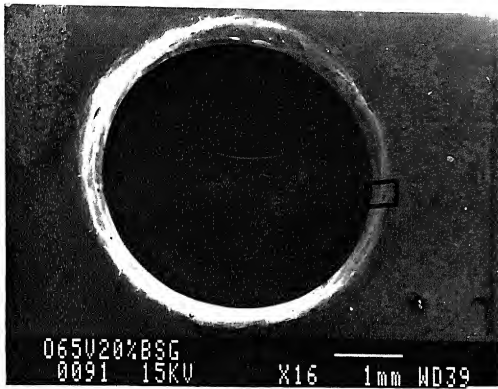
1. Through hole machined in borosilicate glass tube of wall thickness 3 mm in 8.45 minutes at 65 volts with 25 % NaOH. solid eccentric rotational tool is used.

2. Enlarged view of (1) showing thermally damaged zone arround the machined surface.
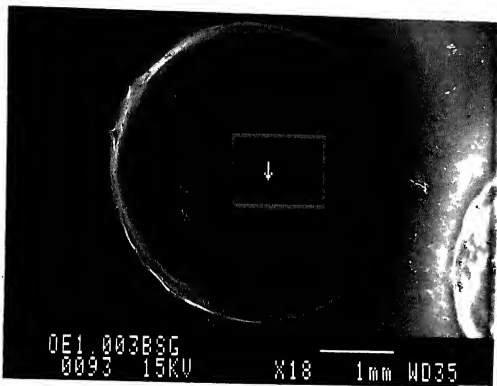
3. Blind hole in borosilicate glass at 65 volts with solid eccentrically rotating tool at 20 rpm.
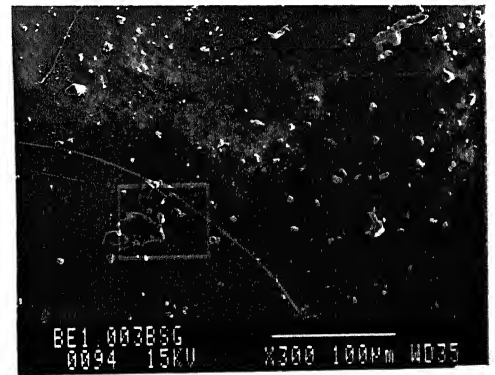
4. Enlarged view of (3) showing resolidified debris at the bottom of the blind hole.

5. Enlarged view of (4) showing details of debris.

6. Blind hole in borosilicate glass with flow of electrolyte through a hollow rotating tool at 20 rpm with 65 volts during 4 minutes machining .
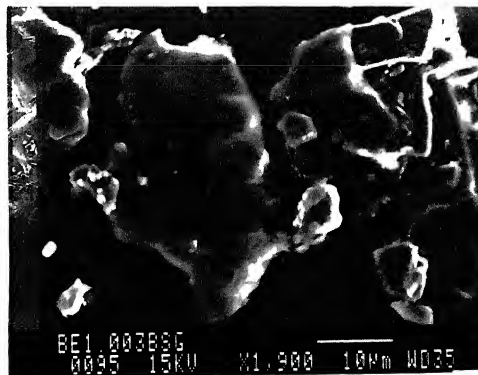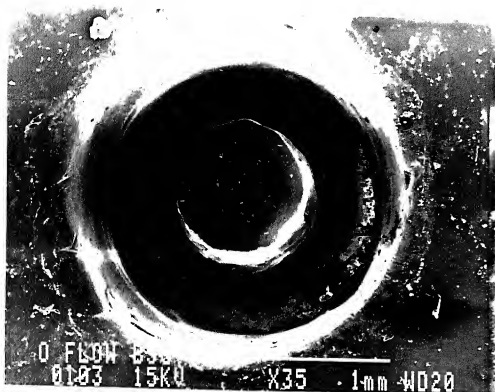
7. Enlarged view of (6) showing bottom portion of hole.
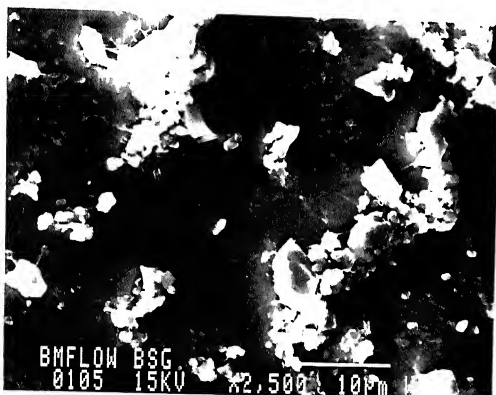
8. Enlarged view of (7) showing details of resolidified debris at the bottom.
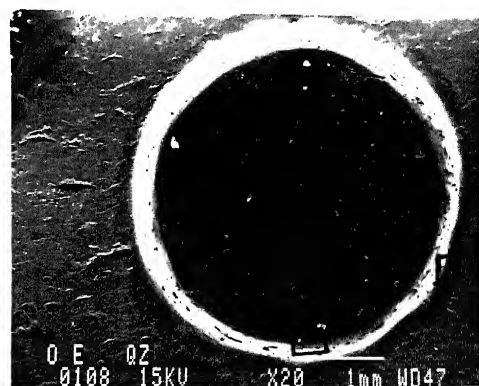
9. Blind hole in quartz at 65 volts during 4 minutes machining with eccentric rotating tool at 20 rpm.
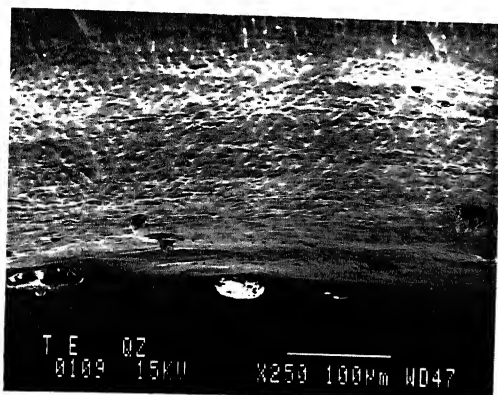
10. Enlarged view of (9) showing thermally damaged zone and resolidified debris on the wall of machined surface
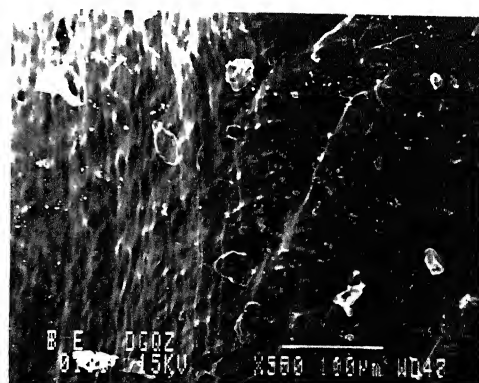
11. Enlarged view of (9) showing comparision of thermally damaged zone by ECD machined surface and diamond grind surface . Few cracks are also visible in the intermediate zone.

work surface.

Figures 3.11(15) and 3.11(17) show the magnified view of striated sub surfaces of the machined hole in borosilicate glass. This surface may be a resultant of the stepped rotation of the tool and non uniform availability of the electrolyte in machining zone. Figure 3.11(20) shows that such surface is absent when stationary tool is used. However, this sub surface generation can not be completely explained. As is evident from the figure 3.11(18,19) that such surface irregularities on the quartz are observed with different pattern. This sub surface generation phenomenon requires further investigation.

3.7.3 Thermal spalling

By and large, it has been accepted that melting is the process of material removal in ECDM, however, based on SEM study, it is also felt that there is some contribution of thermal spalling phenomenon in material removal.

Thermal spalling of a material is usually defined as a mechanical failure of the material, without melting, due to the created internal stresses which overcome the bond strength [26]. This occurs as the material expands or contracts during a sudden temperature change, resulting in tension or compression, sufficient to cause tension or compression failure respectively.

During ECDM process on sudden heating, the material is exposed to high temperature, tries to expand but, is prevented from doing so by the cooler interior material. At the same time, this places the interior material in tension as it is pulled by the outer material which tries to expand. This situation is reversed on sudden cooling. In the present ECDM process, when tool is eccentrically rotated

12. A through hole in borosilicate glass photographed in inclined position , machined at 65 volts during eccentric rotation of tool at 20 rpm
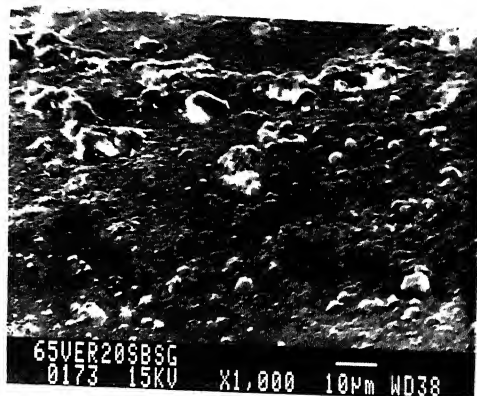
13. Enlarged view of (12) showing ECD machined wall surface and resolidified debris on the wall.
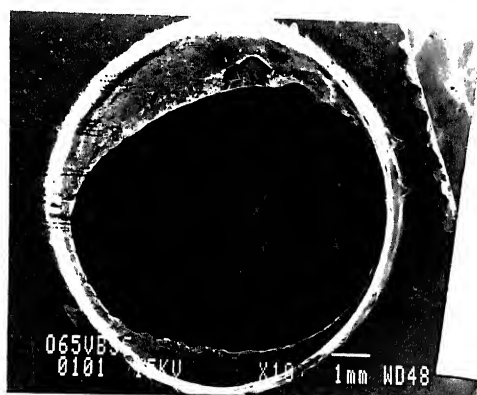
14. Through hole by trepanning in borosilicate glass tube of 3 mm wall thickness at 65 volts during 10.5 minutes machining. Due to curvature of the tube left overs of the sides are visible.
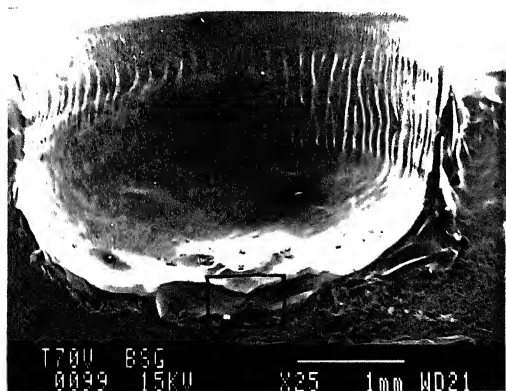
15. Sectioned view of a blind hole ECD machined in a borosilicate glass at 70 volts with eccentric tool rotation at 20 rpm. Striated sur-
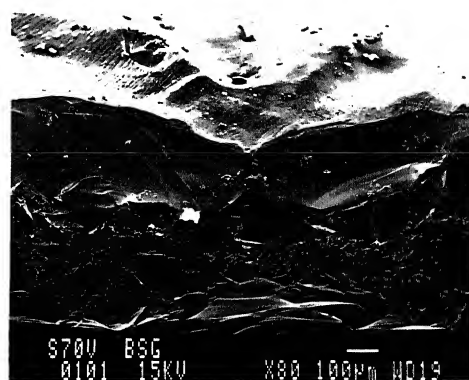
16. Enlarged view of (15) showing bottom portion of the hole. Three different regions are visible.
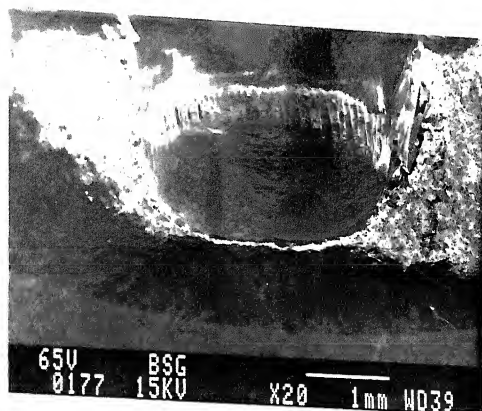
17. Sectioned view of a blind hole ECD machined in a borosilicate glass at 65 volts with eccentric tool rotation at 20 rpm. Striated surface is visible on the wall of the machined surface.
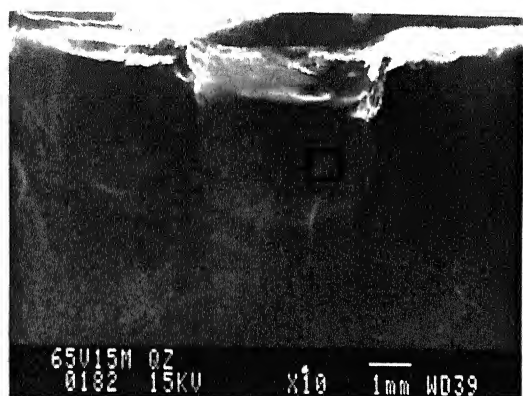
18. Sectioned view of a blind hole machined in quartz during 15 minutes machining at 65 volts.
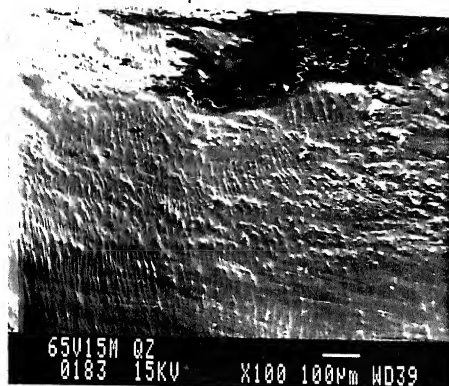
19. Enlarged view of (18) showing striated wall surface.
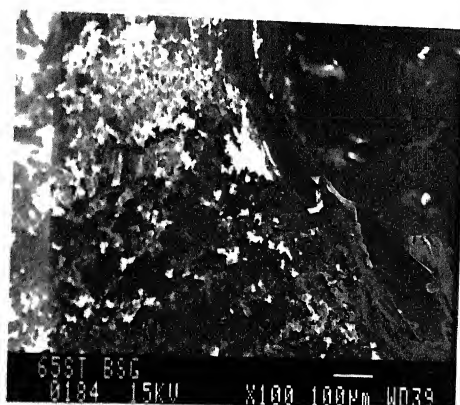
20. Sectioned blind hole in borosilicate glass at 65 volts using solid stationary tool .

Figure 3.11: Contd.

（68）
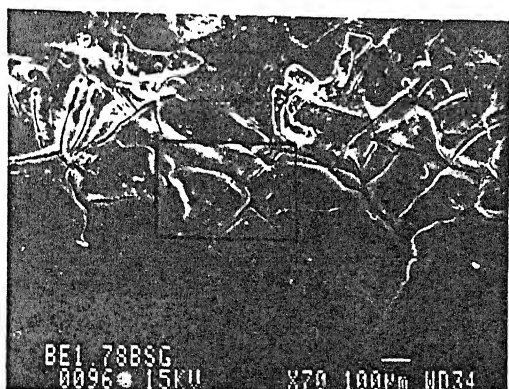
21. Enlarged view of the bottom surface machined with eccentric rotating tool (trepanning) at 65 volts in borosilicate glass.
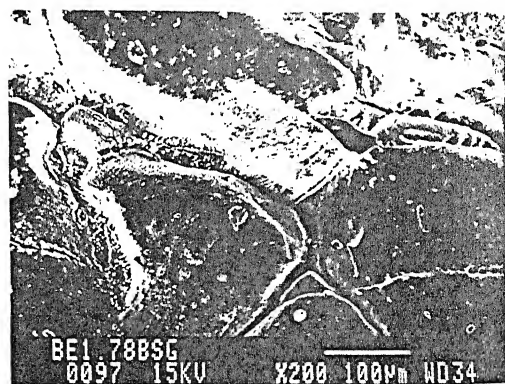
22. Enlarged view of (21) showing spalled and damaged bottom surface during trepanning .
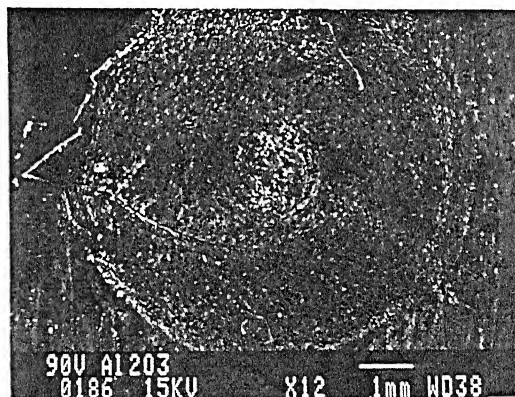
23. Alumina machined with eccentric tool rotating (trepanning) at 90 volts during 15 minutes of machining, 590 μm depth obtained.

24. Alumina machining with eccentric tool rotating (sweeping) at 90 volts during 15 minutes of machining, 750 μm depth obtained.

25. Enlarged view of (24) showing bottom surface of the blind hole.

Figure 3.11

Chapter 4

CONCLUDING REMARKS AND SCOPE FOR THE FUTURE WORK

4.1 Conclusions

In this study, electrochemical discharge machining of non-conducting materials has been carried out, and the following conclusions have been derived.

- ECDM, a very useful process, has been successfully employed for the machining of electrically non-conducting ceramics, such as borosilicate glass, quartz etc.

- Rotation of the tool and flow of the electrolyte have improved the process performance. However, in both the cases, the maxima is attained at there low values, beyond which any further increase in speed or electrolyte flow have adversely affected the process performance.

- The limitation associated, ie limiting value of machined depth, with ECDM, has been over come by the use of orbital rotational tool. It has been possible with out sacrificing the surface quality, to drill the hole as deep as 5 mm.

- SEM analysis has revealed that the quality of the surface obtained after ECDM is also fairly good.

4.2 Scope for the Future Work

- Real time work - tool contact sensing remained a problem during the course of this work. A more efficient contact sensor can be designed and implemented for effective control of the gap between work and tool.

- Metal bonded diamond mounted points, with grit size of the order of twice the bubble size can be employed for constant gap ECDM.

- Detailed study of debris and striated wall surface observed during ECDM can be carried out, which will help in understanding the phenomena of material removal in ECDM.

- Theoretical model should be modified by accounting the thermal spalling and thermochemical effect.

- Pulsed power supply with the pulse time of the order of micro second can be used for increasing the material removal rate and improving the surface finish.

- Flow of electrolyte through hollow tool destablized the discharge. Hence, flushing jet following the tool in the orbital motion can be tried for homogeneous machining with efficient flushing.

REFERENCES & BIBLIOGRAPHY

1. Allesu K. - PhD Dissertation,IIT Kanpur, India, 1988.

2. Allesu K., Muju M.K., Ghosh A. - "Experimental in the ECD machining of non-conducting materials", Proc. of . Symp. for Electro-machining (ISEM), 1989.

3. Basak I. - PhD Dissertation, IIT Kanpur, India, 1992.

4. Belyaev V.V. - "Spall damage modelling and dynamic fracture specificities of ceramics", Juurnal of Mat. Proce. Tech., Vol 32, pp 135-144, 1992.

5. Benedict G.F. - "Non-traditional Manufacturing Processes", Marcel Dekker Inc., 1987.

6. Bifano T.G., DePiero D.K, Golini D. - "Chemomechanical effects in ductile-regime machining of glass", Precision Engineering, Vol. 14, No. 4, pp 238-247, 1993.

7. Chikamori K. - "Grooving of Silicon Nitride Ceramics With ArcDischarge in Electrolyte", Int. Journal of JSPE, Vol. 25, No 2, pp 109-110, 1991

8. Cook N.H., Foote G.B., Jordan P., Kalyani B.N. - "Experimental studies in electromachining", Trans. ASME, Journal of Engg. for Ind., pp 945-950, Nov. 1973.

9. Crichton I.M., McGeoug J.A. - "Studies of the discharge mechanism in electrochemical arc machining", Journal of Applied Electrochemistry, Vol.15, pp 113-119, 1985.

10. Gadalla A.M., Buzkurt B, Faulk N.M., - "Modeling of Thermal Spalling During Electrical Discharge Machinig of Titanium Diboride", J. Am. Ceram. Soc., Vol 74 (4), pp 801-806, 1991

11. Ghosh A. - "Electrochemical DischargeMachining - A New Process with Maney Possibilities", IE(I) Journal -PR, pp 14-18, 1991.

12. Ito S., Nakamura M., Kanematsu - "Machining of High Performacce Ceramics", Bull. of JSPE, Vol. 21, No. 3, pp 167-172, 1987.

13. Jain V.K., Rao P.S., Choudhary S.K. and Rajurkar K.P. - "Experimental investigations into TW-ECSM of composites",Trans. ASME, Journal of Engg. for Ind., pp 75-84, Vol 113, Feb 1991.

14. Komaraiah M., Moman M.A., Reddy P.N., Victor S. - "Investigation of surface roughness and accuracy in ultrasonic machining", Precision Engineering, Vol. 10, No. 2, pp 59-65, 1988.

15. Konig W., Dauw D.F, - "EDM - Future Steps towards the Machining of Ceramics", Annals of the CIRP, Vol. 37/2, pp 623-631, 1988.

16. Kubata M., Tomura Y - "ECDM Drills a Steel Plate With High Feed Rate", Bull of JSPE, Vol. 7, No. 4, p 117, 1973.

17. Kurafugi H., Suda H. - "Electrical Discharge Drilling of Glass", Annals of the CIRP, Vol. 16/I, p 415, 1968.

18. Larsson C.N. and Bauxter E.M. - "Tool damage by sparking in ECM", Proc. of the IMTDR, p 499, 1977.

19. Lee L.C., Lim L.C., Venketash V.C. -"Quantification of surface damage of tool steel after EDM", Int. J. Mach. Tools. Manufact., Vo.28, No.4, pp 359-372, 1988.

20. Loutrel S.P. and Cook N.H. - "High rate electro-chemical machining", Trans. ASME, Journal of Engg. for Ind., Nov., p 992-996, 1973.

21. Mcgeough J. A. - " Principles of electrochemical machining " Chapman and Hall, London 1974.

22. McGeough J.A. - "Advanced Method of Machining" Chapman and Hall, 1988.

23. McGeough J.A. and Crichton I.M. - "Studies of the discharge mechanism in electro-chemical arc machining",Journal of Appl. Electrochemistry , pp 113-119 , 1985.

24. Nesarikar V.V., Jain V.K., Chaudhary S.K. - "Travelling Wire Electrochemical Spark Machining of Thick Sheets of Kaevlar-Epoxy Composites", Proc. of 16th AIMTDR Conf., pp 612, 1994.

25. Nichols P.C. - "Hand book of Ceramics and Composites", Vol 1, McGrall Book Company, 1990.

26. Petrofes N.F., Godalla A.M. - "Electrical Discharge Machining of Advanced Ceramics", Ceramic Bulletin, Vol. 67, No. 6, pp 1048-1052, 1988.

27. Ryshkewitch E. - "Oxide Ceramics", Academic Press, New York, 1960.

28. Shand E.B. - "Glass Engineering Hand Book", McGrall Book Company, 1958.

29. Silva A de, McGough J.A. - "Surface effect on alloys drilled by electrochemical arc machining", Proc. Instn. Mech. Engg., Vol. 200, No. B4, pp 113-119, 1985.

30. Singh Y.P. - "Design and fabricationof TW-ECSM and machining piezoelectric ceramics (PZT)", M.Tech Thesis, IIT Kanpur,

31. Snoeys R., Staelens F.,Dekeyser W. - "Current Trends in Non-Conventional Material Removal Processes", Annals of the CIRP, Vol. 35/II, pp 467-480, 1986.

32. Tandon S., Jain V.K., Kumar P., Rajurkar K.P. - "Investigation into Machining of Composites", Precision Engineering., Vol.12, No.4, pp 225-237, 1990.

33. Tokura H., Kondoh I., Yoshikswa M. - "Ceramic material processing by electrical discharge in electrolyte", J. of Material Science, Vol. 24, pp 991-998, 1989.

34. Tsuchiya H., Inoue T.,Miyazaki M. - "Wire Electro-Chemical Discharge Machining of Glasses and Ceramics", Proc. of 5th ICPE Tokyo, pp 413-417, 1984.

35. Umesh Kumar - "An experimental study of electrical machining of non-conducting materials', M.Tech Thesis, IIT Kanpur, India.

APPENDIX A

Borosilicate Glass

SiO_2	B_2O_3	Al_2O_3	Na_2O_3
80.6%	13 %	2 %	4.4 %

Table A.1: Chemical composition of borosilicate glass

Softening point	$820°C$
Coefficient of thermal expansion	$3.3 \times 10^{-6} K^{-1}$
Specific gravity at $20°C$	2.23
Thermal Conductivity at $20°C$	$1.1304\ Wm^{-1}K^{-1}$

Table A.2: Physical properties of borosilicate glass [28]

APPENDIX B

Quartz

Softening point	$1600°C$
Coefficient of thermal expansion $(20 - 300°C)$	$0.627 \times 10^{-6} K^{-1}$
Specific gravity at $20°C$	2.21
Thermal conductivity	$1.382\ Wm^{-1}K^{-1}$

Table B.1: Physical properties of quartz [29]

Hardness	Silica	Boro silicate	Soda silicate
Rough Polish	2.55	1.56	1
Impact Abrasion	3.6	3.1	1
Diamond Indentation	800	630	530
Knoop	680	550	575

Table B.2: Hardness comparison of various glasses [28]

APPENDIX C

Alumina

Melting point	$2050 \pm 5°C$
Coefficient of thermal expansion $(300°C)$	$2 \times 10^{-3} K^{-1}$
Specific gravity	3.9
Thermal conductivity	$0.0723 \ cal°C^{-1}cm^{-1}sec^{-1}$
Specific heat	$0.206 \ cal°C^{-1}g^{-1}$

Table C.1: Physical properties of sintered alumina [27]

Hardened steel	$1200 - 1500$
Cemented carbide	$1500 - 1800$
Alumina	$2000 - 2200$
Silicon carbide	45000
Boron carbide	7000

Table C.2: Indentation hardness comparison of various materials [27]